Noname manuscript No.
(will be inserted by the editor)

Discrete Adjoint Variable Method for the Sensitivity Analysis of ALI3-P formulations

Álvaro López Varela*, **Corina Sandu, Adrian Sandu and Daniel Dopico***

the date of receipt and acceptance should be inserted later

Abstract In this work, the analytical derivation of the sensitivity analysis of the Augmented Lagrangian Index-3 formulation with velocity and acceleration projections is presented using the discrete adjoint variable method, considering a Newmark's family integrator for the numerical integration of the differential variables and a penalty formulation for the initial acceleration problem. The accuracy and efficiency of the new sensitivity formulation are tested in a five-bar benchmark problem and in a real-life four-wheeled vehicle. The method has been implemented in the multibody library MBSLIM as a general sensitivity formulation for natural and relative coordinate models.

Álvaro López Varela, Daniel Dopico Dopico and Alberto Luaces Fernández
Laboratorio de Ingeniería Mecánica, Universidade da Coruña, Mendizábal s/n, 15403, Ferrol, Spain, E-mail: [alvaro.lopez1,ddopico]@udc.es

1 Introduction

The optimization of the response of dynamic multibody systems (MBS) has been gathering the attention of the multibody community since the inception of the first dynamic formulations [1–3]. Gradient-based optimization methods are usually employed in optimal control or design optimization problems, but they are strongly tied to the properties of the gradient of the objective function [4–6]. The accuracy and efficiency of the sensitivity analysis method used to compute the gradient are crucial to obtain a satisfactory optimum. While poor accuracy may increase the number of optimization iterations or even lead to an erroneous optimum, the CPU time required to compute the gradient will determine the total computational time of the optimization.

The sensitivity analysis of a multibody system can be achieved through different methods. The finite differences method represents the simplest of the differentiation techniques, but it suffers from poor accuracy, high dependency on the magnitude of the perturbation and high computational cost, increasing with the number of parameters [6]. A second option is automatic differentiation, which is a technique that explodes the differentiation capabilities of external libraries [7, 8]. Finally, analytical methods consist in the analytical computation of the derivatives of the dynamic formulation, which usually leads to the best performance in terms of accuracy and computational time, but they have as main drawback a significant increase in the implementation effort compared with other methods.

Analytical sensitivities can be classified into Direct Differentiation Methods (DDM) and Adjoint Variable Methods (AVM) [9] attending to which magnitudes are regarded as the variables of the sensitivity problem. The DDM arises from the direct differentiation of the equations of motion (EoM) of the system, and generates a problem where the sensitivities of the states are the unknowns. The AVM avoids the sensitivities of the states by means of a transformation of the sensitivity problem [10], which highly reduces the gradient computational cost in systems subjected to a high number of parameters.

The derivation of the sensitivity expressions is also conditioned by the order between differentiation and discretization [11, 12]. In the *differentiate-then-discretize* approach, the dynamic expressions are considered as continuous, and a numerical integrator is applied to the sensitivity expressions to solve them. In the *discretize-then-differentiate* approach, the dynamics are regarded as a set of algebraic expressions resulting from the application of a numerical integrator to the EoM of the system. The differentiation process handles derivatives of algebraic expressions, which usually leads to simpler expressions but particular for the numerical integrator used in the dynamics.

Accuracy and efficiency are as important in a sensitivity analysis as in the evaluation of the dynamics. The Augmented Lagrangian Index-3 formulation with projections (ALI3-P) offers high accuracy at position, velocity and acceleration levels with a reduced computational time. From the seminal work by Bayo and Ledesma [13], this formulation has been applied to natural coordinates [14] and relative coordinates models [15, 16] in the field of rigid body dynamics. Moreover, this formalism has been extended to flexible multibody systems [17–19], and its capabilities have been exploited for real time simulation [20, 19]. Recently, the focus has been moved to sensitivity analysis [5, 21].

In this work, the *discretize-then-differentiate* approach is applied to the ALI3-P formulation in the sense of the AVM. The new sensitivity formulation is regarded as a means to reduce the complexity of the continuous method presented in [21]. The method has been implemented in the general purpose multibody library MBSLIM [22] as general sensitivity formulations for the global and topological forward dynamics formulations in natural and relative coordinates presented in [14, 16].

This paper is structured as follows: in section 2, the ALI3-P forward dynamic formulation is briefly outlined; in section 3, the Newmark's family of numerical integrators used to solve the dynamics is introduced; section 4 encompasses the direct sensitivity analysis of the ALI3-P formulation; section 5 includes the main contribution of the paper, which is the derivation of the adjoint variable method using a *discretize-then-differentiate* approach applied to the ALI3-P global and topological formulations; in section 6, the new sensitivity formulation is tested with two numerical experiments, one referred to a benchmark problem and the other to a more complex real-life vehicle; finally, section 7 gathers the conclusions of the present work.

2 Forward dynamic formulation

The performance of a forward dynamic multibody formulation can be measured by three crucial factors, which are accuracy, stability and efficiency. In general, an increase of accuracy and/or stability is to the detriment of efficiency and vice versa. Nevertheless, the augmented Lagrangian ALI3-P formulations conquer good levels of these three properties, guaranteeing accuracy with the imposition of constraints in position, velocity and acceleration, reducing instability by means of velocity and acceleration projections while keeping a low computational cost.

In this section, a brief description of the ALI3-P formulation presented in [14] is exposed. Let us consider a multibody system described by means of $\boldsymbol{\rho} \in \mathbb{R}^p$ parameters and $\mathbf{q} \in \mathbb{R}^n$ generalized dependent coordinates subjected to $\boldsymbol{\Phi} \in \mathbb{R}^m$ holonomic constraints[1]. The classical representation of the augmented Lagrangian index 3-formulation takes the form:

$$\left[\mathbf{M}\ddot{\mathbf{q}}^* + \boldsymbol{\Phi}_{\mathbf{q}}^{\mathrm{T}}\left(\boldsymbol{\lambda}^* + \boldsymbol{\alpha}\boldsymbol{\Phi}\right)\right]^{\{i\}} = \mathbf{Q}^{\{i\}} \tag{1a}$$

$$\boldsymbol{\lambda}^{*\{i+1\}} = \boldsymbol{\lambda}^{*\{i\}} + \boldsymbol{\alpha}\boldsymbol{\Phi}^{\{i\}}; \quad i = 0, 1, 2, \ldots \tag{1b}$$

in which $\mathbf{M}(\mathbf{q},\boldsymbol{\rho}) \in \mathbb{R}^{n\times n}$ is the mass matrix, $\ddot{\mathbf{q}}^* \in \mathbb{R}^n$ the unprojected accelerations, $\boldsymbol{\Phi}_{\mathbf{q}}(\mathbf{q},\boldsymbol{\rho}) \in \mathbb{R}^{m\times n}$ is the Jacobian of the constraints, $\boldsymbol{\lambda}^* \in \mathbb{R}^m$ corresponds to the approximate Lagrange multipliers, $\boldsymbol{\alpha} \in \mathbb{R}^{m\times m}$ is a diagonal matrix which contains the penalty factors associated with each one of the constraints, $\mathbf{Q}(\mathbf{q},\dot{\mathbf{q}}^*,\boldsymbol{\rho}) \in \mathbb{R}^n$ is the vector of generalized forces and the superindex i indicates the iteration index.

Equation (1) delivers the exact values of the Lagrange multipliers $\boldsymbol{\lambda}$ when $i \to \infty$. However, with the appropriate penalty factors, convergence can be reached in a few iterations given the fulfillment of an error criteria. As proposed by Dopico et al. in [14], the initialization of the approximated Lagrange multipliers at the beginning of the iteration process (with $i = 0$) with the values of the previous time step usually speeds up convergence [2].

The augmented Lagrangian index-3 problem is usually solved by means of a Newton-Raphson scheme, with increments in positions as main variables. Computational effort can be reduced through the use of an approximate tangent matrix instead of the exact one, but

[1] For simplicity, only holonomic constraints will be considered in this work, although the ALI3-P formulation presented in [14] supports also non-holonomic constraints.

[2] Aquí hay algo que no habíamos estudiado lo suficiente y es que, cuando hay restricciones redundantes, un factor de reducción de los multiplicadores en torno a 0.8 o 0.9 puede mejorar la convergencia y evitar que los multiplicadores se disparen. Esto lo observó experimentalmente Emilio en un sistema con ecuaciones redundantes y es algo que sabemos pero que está sin estudiar debidamente.

the terms that could be neglected could vary depending on the mechanism or the set of coordinates used to model the system [3].

Another property of the augmented Lagrangian index-3 is the support of redundant constraints, which could eventually arise in the definition of a multibody mechanism or in the combination of the dynamic expressions with others in the sense of a multiphysics problem [4].

The solution of the previous index-3 system with classical integrators, can lead to instabilities related to numerical errors that gradually increment the violation of constraints in velocities and accelerations. There are different techniques to keep these violations bounded without modifying the index of the dynamic equations, such as the use of energy conserving or dissipative numerical integrators or the addition of projections onto the velocity and acceleration constraints manifolds.

The inception of velocity and acceleration projections from a minimization problem [13] is omitted here, and only final expressions are presented. Moreover, only penalty non-iterative projections will be consider in order to simplify the expressions as much as possible regarding the sensitivity analysis of the following sections. The velocities resulting from (1) can be projected onto the velocity constraints manifold with:

$$\left(\bar{\mathbf{P}} + \varsigma \mathbf{\Phi}_{\mathbf{q}}^{\mathrm{T}} \boldsymbol{\alpha} \mathbf{\Phi}_{\mathbf{q}}\right) \dot{\mathbf{q}} = \bar{\mathbf{P}} \dot{\mathbf{q}}^{*} - \mathbf{\Phi}_{\mathbf{q}}^{\mathrm{T}} \varsigma \boldsymbol{\alpha} \mathbf{\Phi}_{t} \tag{2}$$

where $\bar{\mathbf{P}} \in \mathbb{R}^{n \times n}$ is a symmetric projection matrix and ς is a penalty factor.

Similarly, unprojected accelerations can be projected onto the acceleration constraints manifold using:

$$\left(\bar{\mathbf{P}} + \varsigma \mathbf{\Phi}_{\mathbf{q}}^{\mathrm{T}} \boldsymbol{\alpha} \mathbf{\Phi}_{\mathbf{q}}\right) \ddot{\mathbf{q}} = \bar{\mathbf{P}} \ddot{\mathbf{q}}^{*} - \mathbf{\Phi}_{\mathbf{q}}^{\mathrm{T}} \varsigma \boldsymbol{\alpha} \left(\dot{\mathbf{\Phi}}_{\mathbf{q}} \dot{\mathbf{q}} + \dot{\mathbf{\Phi}}_{t}\right) \tag{3}$$

The mass matrix is usually used as projection matrix delivering the so called mass orthogonal projections. This seems to be a good choice regarding that this matrix is always symmetric and semi-defined positive and that the resulting projections are unconditionally dissipative, this is, do not add spurious energy to the system, as it was demonstrated by García Orden and Dopico in [23] for positive definite mass matrices. This result can be easily extended to semi-definite mass matrices, attending to the fact that a variation on the additional massless variables do not change the kinetic energy of the system.

In general, velocity projections are sufficient to stabilize an index-3 formulation, but numerical experiments indicate that acceleration projections enhance convergence with a minimum additional cost, since the factorization of the velocity projection system matrix can be directly reused on the acceleration problem. Additionally, projections can be executed only under certain conditions of the constraint time derivatives violation, which contributes to minimize the computational effort without damaging accuracy or stability.

3 Numerical integrator

The EoM presented in the previous section are not analytically solvable for any multibody system, but they require a numerical integrator to be solved. There are multiple numerical integrators that have been applied to multibody systems, and there is no consensus regarding which one delivers the best performance in terms of CPU time, accuracy and stability.

One of the most popular numerical integrators in the multibody community is the Newmark integrator, which spans a series of numerical integrators for second order differential

[3] ¿No podemos funcionar siempre con la matriz típica aproximada?.
[4] WHY?

equations. The performance of these integrators is conditioned by two parameters, γ and β, whose values determine not only their stability, but the energy dissipation and the order of accuracy.

Considering positions as main variables, these numerical integrators take the form:

$$\dot{\mathbf{q}}_{n+1} = \frac{\gamma}{\beta h}\mathbf{q}_{n+1} + \hat{\dot{\mathbf{q}}}_n; \qquad \hat{\dot{\mathbf{q}}}_n = -\left(\frac{\gamma}{\beta h}\mathbf{q}_n + \left(\frac{\gamma}{\beta} - 1\right)\dot{\mathbf{q}}_n + \left(\frac{\gamma}{2\beta} - 1\right)h\ddot{\mathbf{q}}_n\right) \tag{4a}$$

$$\ddot{\mathbf{q}}_{n+1} = \frac{1}{\beta h^2}\mathbf{q}_{n+1} + \hat{\ddot{\mathbf{q}}}_n; \qquad \hat{\ddot{\mathbf{q}}}_n = -\left(\frac{1}{\beta h^2}\mathbf{q}_n + \frac{1}{\beta h}\dot{\mathbf{q}}_n + \left(\frac{1}{2\beta} - 1\right)\ddot{\mathbf{q}}_n\right) \tag{4b}$$

Although equations (4) have the same expressions for all the Newmark family of integrators, the selection of γ and β lead to completely different behaviors. Considering $\gamma = 1/2$ and $\beta = 1/4$, equations of the trapezoidal rule are reached, with its well known properties of A-stability, second order accuracy and energy conservation for linear systems.

Besides, these parameters can be modified so as to add numerical dissipation to the solution, which sometimes is useful to stabilize it. Dissipative Newmark integrators are usually build around one parameter ξ, with γ and β:

$$\gamma = \frac{(1-\xi)^2}{4},\ \beta = \frac{1-2\xi}{2},\ \text{with } \xi < 0. \tag{5}$$

4 Direct sensitivity analysis

Prior to immerse ourselves in the development of the sensitivity analysis, let us define an objective function $\boldsymbol{\psi} \in \mathbb{R}^o$ dependent on the states $\mathbf{q}$, $\dot{\mathbf{q}}$ and $\ddot{\mathbf{q}}$, the Lagrange multipliers $\boldsymbol{\lambda}^*$ and the set of parameters $\boldsymbol{\rho}$.

$$\boldsymbol{\psi} = \int_{t_F}^{t_0} \mathbf{g}\left(\mathbf{q}, \dot{\mathbf{q}}, \ddot{\mathbf{q}}, \boldsymbol{\lambda}^*, \boldsymbol{\rho}\right) \mathrm{dt} \tag{6}$$

Taking derivatives of (6), the gradient of the objective function with respect to the set of parameters leads to:

$$\boldsymbol{\psi}' = \nabla \boldsymbol{\psi}^T = \int_{t_F}^{t_0} \left(\mathbf{g}_{\mathbf{q}}\mathbf{q}' + \mathbf{g}_{\dot{\mathbf{q}}}\dot{\mathbf{q}}' + \mathbf{g}_{\ddot{\mathbf{q}}}\ddot{\mathbf{q}}' + \mathbf{g}_{\boldsymbol{\lambda}^*}\boldsymbol{\lambda}^{*\prime} + \mathbf{g}_{\boldsymbol{\rho}}\right) \mathrm{dt} \tag{7}$$

In equation (7) the derivatives of g are known, and the terms $\mathbf{q}'$, $\dot{\mathbf{q}}'$, $\ddot{\mathbf{q}}'$ and $\boldsymbol{\lambda}^{*\prime}$ are the unknown sensitivity variables, which can be obtained from the sensitivity analysis of the EoM.

Considering the ALI3-P formulation, its sensitivity analysis can be obtained applying the DDM to the continuous expressions, as described in [5]. The forward sensitivity expressions developed in this paper are directly presented here in order to establish the base to build the adjoint variable method.

The application of the DDM to (1) leads to a set of p systems of Differential Algebraic Equations (DAE).

$$\left[\mathbf{M}\ddot{\mathbf{q}}^{*\prime} + \mathbf{C}\dot{\mathbf{q}}^{*\prime} + \bar{\mathbf{K}}\mathbf{q}' + \boldsymbol{\Phi}_{\mathbf{q}}^{\mathrm{T}}\boldsymbol{\lambda}^{*\prime}\right]^{\{i\}} = \bar{\mathbf{Q}}^{\boldsymbol{\rho}\{i\}} \tag{8a}$$

$$\boldsymbol{\lambda}^{*\prime\{i+1\}} = \boldsymbol{\lambda}^{*\prime\{i\}} + \boldsymbol{\alpha}\boldsymbol{\Phi}'^{\{i\}} \tag{8b}$$

in which:

$$\bar{\mathbf{K}} = \mathbf{M}_{\mathbf{q}}\ddot{\mathbf{q}}^* + \boldsymbol{\Phi}_{\mathbf{qq}}^{\mathrm{T}}\left(\boldsymbol{\lambda}^* + \boldsymbol{\alpha}\boldsymbol{\Phi}\right) + \boldsymbol{\Phi}_{\mathbf{q}}^{\mathrm{T}}\boldsymbol{\alpha}\boldsymbol{\Phi}_{\mathbf{q}} + \mathbf{K} \tag{9a}$$

$$\bar{\mathbf{Q}}^{\boldsymbol{\rho}} = \mathbf{Q}_{\boldsymbol{\rho}} - \mathbf{M}_{\boldsymbol{\rho}}\ddot{\mathbf{q}}^* - \boldsymbol{\Phi}_{\mathbf{q}\boldsymbol{\rho}}^{\mathrm{T}}\left(\boldsymbol{\lambda}^* + \boldsymbol{\alpha}\boldsymbol{\Phi}\right) - \boldsymbol{\Phi}_{\mathbf{q}}^{\mathrm{T}}\boldsymbol{\alpha}\boldsymbol{\Phi}_{\boldsymbol{\rho}} \tag{9b}$$

$$\boldsymbol{\Phi}' = \boldsymbol{\Phi}_{\mathbf{q}}\mathbf{q}' + \boldsymbol{\Phi}_{\boldsymbol{\rho}} \tag{9c}$$

In (8) and (9), $\mathbf{K} = -\dfrac{\partial \mathbf{Q}}{\partial \mathbf{q}} \in \mathbb{R}^{n\times n}$ and $\mathbf{C} = -\dfrac{\partial \mathbf{Q}}{\partial \dot{\mathbf{q}}} \in \mathbb{R}^{n\times n}$ represent the equivalent stiffness and damping matrices of the system respectively.

The sensitivity analysis of the velocity projections delivers p systems of algebraic equations with the form:

$$\left(\bar{\mathbf{P}} + \varsigma\boldsymbol{\Phi}_{\mathbf{q}}^{\mathrm{T}}\boldsymbol{\alpha}\boldsymbol{\Phi}_{\mathbf{q}}\right)\dot{\mathbf{q}}' = \bar{\mathbf{P}}\dot{\mathbf{q}}^{*\prime} + \bar{\mathbf{P}}'\left(\dot{\mathbf{q}}^* - \dot{\mathbf{q}}\right) - \left(\boldsymbol{\Phi}_{\mathbf{qq}}^{\mathrm{T}}\varsigma\boldsymbol{\alpha}\dot{\boldsymbol{\Phi}}\right)\mathbf{q}' - \boldsymbol{\Phi}_{\mathbf{q}\boldsymbol{\rho}}^{\mathrm{T}}\varsigma\boldsymbol{\alpha}\dot{\boldsymbol{\Phi}} - \boldsymbol{\Phi}_{\mathbf{q}}^{\mathrm{T}}\varsigma\boldsymbol{\alpha}\mathbf{b}^{\boldsymbol{\rho}} \tag{10}$$

with:

$$\mathbf{b}^{\boldsymbol{\rho}} = \dot{\boldsymbol{\Phi}}_{\mathbf{q}}\mathbf{q}' + \dot{\boldsymbol{\Phi}}_{\boldsymbol{\rho}} \tag{11a}$$

$$\bar{\mathbf{P}}' = \bar{\mathbf{P}}_{\mathbf{q}}\mathbf{q}' + \bar{\mathbf{P}}_{\dot{\mathbf{q}}^*}\dot{\mathbf{q}}^{*\prime} + \bar{\mathbf{P}}_{\boldsymbol{\rho}} \tag{11b}$$

Observe that in the case of mass orthogonal projections, the term $\bar{\mathbf{P}}_{\dot{\mathbf{q}}^*}$ vanishes.

Similarly to velocity projections, the sensitivity analysis of acceleration projections leads to other p systems of algebraic equations:

$$\left(\bar{\mathbf{P}} + \varsigma\boldsymbol{\Phi}_{\mathbf{q}}^{\mathrm{T}}\boldsymbol{\alpha}\boldsymbol{\Phi}_{\mathbf{q}}\right)\ddot{\mathbf{q}}' = \bar{\mathbf{P}}\ddot{\mathbf{q}}^{*\prime} + \bar{\mathbf{P}}'\left(\ddot{\mathbf{q}}^* - \ddot{\mathbf{q}}\right) - \left(\boldsymbol{\Phi}_{\mathbf{qq}}^{\mathrm{T}}\varsigma\boldsymbol{\alpha}\ddot{\boldsymbol{\Phi}}\right)\mathbf{q}' - \boldsymbol{\Phi}_{\mathbf{q}\boldsymbol{\rho}}^{\mathrm{T}}\varsigma\boldsymbol{\alpha}\ddot{\boldsymbol{\Phi}} - \boldsymbol{\Phi}_{\mathbf{q}}^{\mathrm{T}}\varsigma\boldsymbol{\alpha}\mathbf{c}^{\boldsymbol{\rho}} \tag{12}$$

with:

$$\mathbf{c}^{\boldsymbol{\rho}} = 2\dot{\boldsymbol{\Phi}}_{\mathbf{q}}\dot{\mathbf{q}}' + \ddot{\boldsymbol{\Phi}}_{\mathbf{q}}\mathbf{q}' + \ddot{\boldsymbol{\Phi}}_{\boldsymbol{\rho}} \tag{13}$$

Note that the sensitivities of the velocity coordinates used in the acceleration projections are the result of the sensitivities of the velocity projections, and not the unprojented velocity sensitivities.

As it can be deduced from equations (8), (10) and (12), the number of systems to be solved grows linearly with the number of parameters. Even though only two tangent matrices have to be factorized per time step (one for (8) and other for (10) and (12)), the number of systems are detrimental to the efficiency of the method. In the case of a high number of parameters, the AVM should be used instead of the DDM.

5 Discrete adjoint variable method

The AVM is a well known technique to compute the sensitivity analysis of a set of equations avoiding the sensitivities of the original variables. This method is widely spread in the multibody community, specially in control applications, where the number of parameters (or equivalent magnitudes) is high. From the point of view of the order between differentiation and discretization, the AVM can be classified in two groups: Continuous Adjoint Variable Methods (CAVM) and Discrete Adjoint variable methods (DAVM) [24].

In CAVM, the EoM are regarded as continuous in time, and the set of adjoint equations generated preserves the structure of the original set of equations (if the original equation is a index-3 DAE, the adjoint equations will be a index-3 DAE too). This method usually exploits the integration by parts to eliminate the sensitivities of the time derivatives of the states, which generates a set of conditions at the initial and final time. Even though the conditions at the initial time t_0 does not involve special problems (the sensitivities of the states can be easily computed at the initial instant of time by means of kinematic sensitivity problems), final conditions usually lead to a complex initialization process, and often a set of new adjoint variables have to be resorted to initialize properly the adjoint variables, as in [9]. In addition, high order time derivatives of some dynamic terms arise from the integration by parts process, none of them being required on the dynamics. This last problem is usually addressed by means of a change of variable [21], or just exploiting the properties of a particular set of coordinates (natural coordinates has a constant mass matrix, being its time derivatives all null).

The shortcomings of the CAVM can be avoided by the use of the DAVM. In this sense, the discrete dynamic expressions at each time step are employed to build the adjoint Lagrangian, generating a set of algebraic adjoint equations with discrete dependencies among instants of time. The relation between consecutive time steps depends on the numerical integrator used, which forces the DAVM to have a different expression for each numerical integrator, being this one of the main drawbacks of the method. However, the initialization process is almost straightforward, there is no need for additional adjoint variables out of the ones related to the dynamic equations and no high order time derivatives are required. The approach has been successfully applied to multibody models in [25] with a Runge-Kutta integrator and in [11,26] with Hilber-Hughes-Taylor integrator, among others.

The application of the CAVM and DAVM to the ALI3-P formulation constitutes a perfect example of the commented problems. The recently published (continuous) adjoint sensitivity of the ALI3-P formulation [21] describes thoroughly the set of transformations required to consistently define the adjoint system of equations, and not only this, but the initialization of the adjoint variables too. The DAVM presented hereinafter solves some of the issues of the CAVM, with the counterpart of limiting the generality of the set of equations generated to the Newmark's family integrator.

First of all, the discrete nature of the DAVM implies that any integral will be substituted by its discrete form in terms of sums. For simplicity, the integral function is discretized by means of the trapezoidal rule, with the form:

$$\int_{t_0}^{t_F} \mathbf{X}\mathrm{dt} = \frac{h}{2}\left(\mathbf{X}_0 + \mathbf{X}_n\right) + h\sum_{i=1}^{n-1}\mathbf{X}_i \tag{14}$$

where h is the time step of the discretization, $n = \frac{t_F - t_0}{h}$ the number of steps and $\mathbf{X}_i$ the value of $\mathbf{X}$ at the time $ih + t_0$.

Accordingly, the cost function (6) can be discretized and transformed into:

$$\boldsymbol{\psi} = \frac{h}{2}\left(\mathbf{g}_0\left(\mathbf{q}_0, \dot{\mathbf{q}}_0, \ddot{\mathbf{q}}_0, \boldsymbol{\lambda}_0^*, \boldsymbol{\rho}\right) + \mathbf{g}_n\left(\mathbf{q}_n, \dot{\mathbf{q}}_n, \ddot{\mathbf{q}}_n, \boldsymbol{\lambda}_n^*, \boldsymbol{\rho}\right)\right) + h\sum_{i=1}^{n-1}\mathbf{g}_i\left(\mathbf{q}_i, \dot{\mathbf{q}}_i, \ddot{\mathbf{q}}_i, \boldsymbol{\lambda}_i^*, \boldsymbol{\rho}\right) \tag{15}$$

In this approach, the index-3 DAE is better suited for building the adjoint system than the Augmented Lagrangian index-3 DAE as long as it does not require an iteration for the Lagrange multipliers. The lemma 4.3 presented in [21] establishes the base to interchange these two formulations within a sensitivity analysis, using the following upgrade of the Lagrange multipliers:

$$\boldsymbol{\lambda} \approx \left(\boldsymbol{\lambda}^* + \boldsymbol{\alpha}\boldsymbol{\Phi}\right) \tag{16}$$

where $\boldsymbol{\lambda}$ are the Lagrange multipliers of the index-3 DAE and $\boldsymbol{\lambda}^*$ are the approximated ones of the Augmented Lagrange index-3.

The index-3 DAE tangent linear model (TLM) here considered is:

$$\mathbf{M}\ddot{\mathbf{q}}^{*\prime} + \mathbf{C}\dot{\mathbf{q}}^{*\prime} + \left(\mathbf{M}_{\mathbf{q}}\ddot{\mathbf{q}}^{*} + \mathbf{\Phi}_{\mathbf{qq}}^{\mathrm{T}}\boldsymbol{\lambda} + \mathbf{K}\right)\mathbf{q}' + \mathbf{\Phi}_{\mathbf{q}}^{\mathrm{T}}\boldsymbol{\lambda}' = \mathbf{Q}_{\boldsymbol{\rho}}^{d} - \mathbf{M}_{\boldsymbol{\rho}}\ddot{\mathbf{q}}^{*} - \mathbf{\Phi}_{\mathbf{q}\boldsymbol{\rho}}^{\mathrm{T}}\boldsymbol{\lambda} \tag{17a}$$

$$\mathbf{\Phi}_{\mathbf{q}}\mathbf{q}' = -\mathbf{\Phi}_{\boldsymbol{\rho}} \tag{17b}$$

and with the substitution of the Lagrange multipliers by the ones of the Augmented Lagrange scheme:

$$\begin{aligned}\mathbf{M}\ddot{\mathbf{q}}^{*\prime} + \mathbf{C}\dot{\mathbf{q}}^{*\prime} + \left(\mathbf{M}_{\mathbf{q}}\ddot{\mathbf{q}}^{*} + \mathbf{\Phi}_{\mathbf{q}}^{\mathrm{T}}\boldsymbol{\alpha}\mathbf{\Phi}_{\mathbf{q}} + \mathbf{\Phi}_{\mathbf{qq}}^{\mathrm{T}}\left(\boldsymbol{\lambda}^{*} + \boldsymbol{\alpha}\mathbf{\Phi}\right) + \mathbf{K}\right)\mathbf{q}' + \mathbf{\Phi}_{\mathbf{q}}^{\mathrm{T}}\boldsymbol{\lambda}^{*\prime} = \\ \mathbf{Q}_{\boldsymbol{\rho}} - \mathbf{M}_{\boldsymbol{\rho}}\ddot{\mathbf{q}}^{*} - \mathbf{\Phi}_{\mathbf{q}\boldsymbol{\rho}}^{\mathrm{T}}\left(\boldsymbol{\lambda}^{*} + \boldsymbol{\alpha}\mathbf{\Phi}\right) - \mathbf{\Phi}_{\mathbf{q}}^{\mathrm{T}}\boldsymbol{\alpha}\mathbf{\Phi}_{\boldsymbol{\rho}}\end{aligned} \tag{18a}$$

$$\mathbf{\Phi}_{\mathbf{q}}\mathbf{q}' = -\mathbf{\Phi}_{\boldsymbol{\rho}} \tag{18b}$$

The discrete approach used to solve the dynamics require to handle the derivatives of the equations with the numerical integrator already applied to them. In the present development, the Newmark's integrator is selected as numerical integrator due to its simplicity and good behavior, with the sensitivities of positions of the states considered as the main variables of the system. The application of the integrator to the index-3 DAE TLM yields:

$$\begin{aligned}\left(\mathbf{M}_{\mathbf{q}}\ddot{\mathbf{q}}^{*} + \mathbf{\Phi}_{\mathbf{q}}^{\mathrm{T}}\boldsymbol{\alpha}\mathbf{\Phi}_{\mathbf{q}} + \mathbf{\Phi}_{\mathbf{qq}}^{\mathrm{T}}\left(\boldsymbol{\lambda}^{*} + \boldsymbol{\alpha}\mathbf{\Phi}\right) + \mathbf{K} + \frac{1}{\beta h}\mathbf{M} + \frac{\gamma}{\beta h}\mathbf{C}\right)\mathbf{q}^{*\prime} + \mathbf{\Phi}_{\mathbf{q}}^{\mathrm{T}}\boldsymbol{\lambda}^{*\prime} = \\ \mathbf{Q}_{\boldsymbol{\rho}} - \mathbf{M}_{\boldsymbol{\rho}}\ddot{\mathbf{q}}^{*} - \mathbf{\Phi}_{\mathbf{q}\boldsymbol{\rho}}^{\mathrm{T}}\left(\boldsymbol{\lambda}^{*} + \boldsymbol{\alpha}\mathbf{\Phi}\right) - \mathbf{\Phi}_{\mathbf{q}}^{\mathrm{T}}\boldsymbol{\alpha}\mathbf{\Phi}_{\boldsymbol{\rho}} - \mathbf{M}\hat{\ddot{\mathbf{q}}}' - \mathbf{C}\hat{\dot{\mathbf{q}}}'\end{aligned} \tag{19a}$$

$$\mathbf{\Phi}_{\mathbf{q}}\mathbf{q}' = -\mathbf{\Phi}_{\boldsymbol{\rho}} \tag{19b}$$

in which the equations of the Newmark integrator (4) have been extended to sensitivities.

The application of the numerical integrator to the sensitivities of the velocity projections yields:

$$\left(\bar{\mathbf{P}} + \varsigma\mathbf{\Phi}_{\mathbf{q}}^{\mathrm{T}}\boldsymbol{\alpha}\mathbf{\Phi}_{\mathbf{q}}\right)\dot{\mathbf{q}}' = \bar{\mathbf{P}}\left(\frac{\gamma}{\beta h}\mathbf{q}' + \hat{\dot{\mathbf{q}}}'\right) + \bar{\mathbf{P}}'\left(\dot{\mathbf{q}}^{*} - \dot{\mathbf{q}}\right) - \left(\mathbf{\Phi}_{\mathbf{qq}}^{\mathrm{T}}\varsigma\boldsymbol{\alpha}\dot{\mathbf{\Phi}}\right)\mathbf{q}' - \mathbf{\Phi}_{\mathbf{q}\boldsymbol{\rho}}^{\mathrm{T}}\varsigma\boldsymbol{\alpha}\dot{\mathbf{\Phi}} - \mathbf{\Phi}_{\mathbf{q}}^{\mathrm{T}}\varsigma\boldsymbol{\alpha}\mathbf{b}^{\boldsymbol{\rho}} \tag{20}$$

Similarly, the sensitivities of the acceleration projections are:

$$\left(\bar{\mathbf{P}} + \varsigma\mathbf{\Phi}_{\mathbf{q}}^{\mathrm{T}}\boldsymbol{\alpha}\mathbf{\Phi}_{\mathbf{q}}\right)\ddot{\mathbf{q}}' = \bar{\mathbf{P}}\left(\frac{1}{\beta h^{2}}\mathbf{q}' + \hat{\ddot{\mathbf{q}}}'\right) + \bar{\mathbf{P}}'\left(\ddot{\mathbf{q}}^{*} - \ddot{\mathbf{q}}\right) - \left(\mathbf{\Phi}_{\mathbf{qq}}^{\mathrm{T}}\varsigma\boldsymbol{\alpha}\ddot{\mathbf{\Phi}}\right)\mathbf{q}' - \mathbf{\Phi}_{\mathbf{q}\boldsymbol{\rho}}^{\mathrm{T}}\varsigma\boldsymbol{\alpha}\ddot{\mathbf{\Phi}} - \mathbf{\Phi}_{\mathbf{q}}^{\mathrm{T}}\varsigma\boldsymbol{\alpha}\mathbf{c}^{\boldsymbol{\rho}} \tag{21}$$

The first step in the generation of the adjoint equations is the composition of a Lagrangian preserving the same value of the objective function but including a set of new adjoint variables. To keep the notation as clear as possible, let us define the Lagrangian at an instant of time t_i such as:

$$\begin{aligned}\mathscr{L}_i = \boldsymbol{\psi} - \boldsymbol{\mu}^{\mathrm{T}}\left(\mathbf{M}\ddot{\mathbf{q}}^{*} + \mathbf{\Phi}_{\mathbf{q}}^{\mathrm{T}}\left(\boldsymbol{\lambda}^{*} + \boldsymbol{\alpha}\mathbf{\Phi}\right) - \mathbf{Q}\right) - \boldsymbol{\mu}_{\mathbf{\Phi}}^{\mathrm{T}}\mathbf{\Phi} \\ -\boldsymbol{\mu}_{\dot{\mathbf{\Phi}}}^{\mathrm{T}}\left(\left[\bar{\mathbf{P}} + \varsigma\mathbf{\Phi}_{\mathbf{q}}^{\mathrm{T}}\boldsymbol{\alpha}\mathbf{\Phi}_{\mathbf{q}}\right]\dot{\mathbf{q}} - \bar{\mathbf{P}}\dot{\mathbf{q}}^{*} + \mathbf{\Phi}_{\mathbf{q}}^{\mathrm{T}}\varsigma\boldsymbol{\alpha}\mathbf{\Phi}_{t}\right) - \\ -\boldsymbol{\mu}_{\ddot{\mathbf{\Phi}}}^{\mathrm{T}}\left(\left[\bar{\mathbf{P}} + \varsigma\mathbf{\Phi}_{\mathbf{q}}^{\mathrm{T}}\boldsymbol{\alpha}\mathbf{\Phi}_{\mathbf{q}}\right]\ddot{\mathbf{q}} - \bar{\mathbf{P}}\ddot{\mathbf{q}}^{*} + \mathbf{\Phi}_{\mathbf{q}}\varsigma\boldsymbol{\alpha}\left(\dot{\mathbf{\Phi}}_{\mathbf{q}}\dot{\mathbf{q}} + \dot{\mathbf{\Phi}}_{t}\right)\right)\end{aligned} \tag{22}$$

in which:

- $\boldsymbol{\mu} \in \mathbb{R}^{n \times o}$ is the set of adjoint variables associated to the first n equations of the index-3 DAE system.

- $\boldsymbol{\mu}_{\boldsymbol{\Phi}} \in \mathbb{R}^{m \times o}$ are the adjoint variables associated to the last m equations of the index-3 DAE system.
- $\boldsymbol{\mu}_{\dot{\boldsymbol{\Phi}}} \in \mathbb{R}^{m \times o}$ is the set of adjoint variables related to the velocity projections.
- $\boldsymbol{\mu}_{\ddot{\boldsymbol{\Phi}}} \in \mathbb{R}^{m \times o}$ is the set of adjoint variables correspondent to acceleration projections.

The gradient of this instant Lagrangian, considering now the discrete derivatives introduced in (18), (20) and (21), has the following expression:

$$
\begin{aligned}
\mathscr{L}_i' = \boldsymbol{\psi}' - \Bigg\{ \boldsymbol{\mu}^{\mathrm{T}} \left(\frac{1}{\beta h^2} \mathbf{M} + \frac{\gamma}{\beta h} \bar{\mathbf{C}} + \bar{\mathbf{K}} \right) \\
+ \boldsymbol{\mu}_{\dot{\boldsymbol{\Phi}}}^{\mathrm{T}} \left(-\bar{\mathbf{P}} \frac{\gamma}{\beta h} - \bar{\mathbf{P}}_{\mathbf{q}} \left(\dot{\mathbf{q}}^* - \dot{\mathbf{q}} \right) + \boldsymbol{\Phi}_{\mathbf{qq}}^{\mathrm{T}} \varsigma \boldsymbol{\alpha} \dot{\boldsymbol{\Phi}} + \boldsymbol{\Phi}_{\mathbf{q}}^{\mathrm{T}} \varsigma \boldsymbol{\alpha} \left(\boldsymbol{\Phi}_{\mathbf{qq}} \dot{\mathbf{q}} + \boldsymbol{\Phi}_{\mathbf{q}t} \right) \right) \\
+ \boldsymbol{\mu}_{\ddot{\boldsymbol{\Phi}}}^{\mathrm{T}} \left(-\bar{\mathbf{P}} \frac{1}{\beta h^2} - \bar{\mathbf{P}}_{\mathbf{q}} \left(\ddot{\mathbf{q}}^* - \ddot{\mathbf{q}} \right) + \boldsymbol{\Phi}_{\mathbf{qq}}^{\mathrm{T}} \varsigma \boldsymbol{\alpha} \ddot{\boldsymbol{\Phi}} + \boldsymbol{\Phi}_{\mathbf{q}}^{\mathrm{T}} \varsigma \boldsymbol{\alpha} \left(\boldsymbol{\Phi}_{\mathbf{qq}} \ddot{\mathbf{q}} + \dot{\boldsymbol{\Phi}}_{\mathbf{qq}} \dot{\mathbf{q}} + \dot{\boldsymbol{\Phi}}_{\mathbf{q}t} \right) \right) + \boldsymbol{\mu}_{\boldsymbol{\Phi}}^{\mathrm{T}} \boldsymbol{\Phi}_{\mathbf{q}} \Bigg\} \mathbf{q}' \\
- \left\{ \boldsymbol{\mu}_{\dot{\boldsymbol{\Phi}}}^{\mathrm{T}} \left(\bar{\mathbf{P}} + \varsigma \boldsymbol{\Phi}_{\mathbf{q}}^{\mathrm{T}} \boldsymbol{\alpha} \boldsymbol{\Phi}_{\mathbf{q}} \right) + \boldsymbol{\mu}_{\ddot{\boldsymbol{\Phi}}}^{\mathrm{T}} \left(\boldsymbol{\Phi}_{\mathbf{q}}^{\mathrm{T}} \varsigma \boldsymbol{\alpha} \left(\boldsymbol{\Phi}_{\mathbf{qq}} \dot{\mathbf{q}} + \dot{\boldsymbol{\Phi}}_{\mathbf{q}} + \boldsymbol{\Phi}_{\mathbf{q}t} \right) \right) \right\} \dot{\mathbf{q}}' \\
- \left\{ \boldsymbol{\mu}_{\ddot{\boldsymbol{\Phi}}}^{\mathrm{T}} \left(\bar{\mathbf{P}} + \varsigma \boldsymbol{\Phi}_{\mathbf{q}}^{\mathrm{T}} \boldsymbol{\alpha} \boldsymbol{\Phi}_{\mathbf{q}} \right) \right\} \ddot{\mathbf{q}}' \\
- \left\{ \left(\boldsymbol{\mu}^{\mathrm{T}} \mathbf{C} - \boldsymbol{\mu}_{\dot{\boldsymbol{\Phi}}}^{\mathrm{T}} \bar{\mathbf{P}} \right) \right\} \hat{\dot{\mathbf{q}}}' \\
- \left\{ \left(\boldsymbol{\mu}^{\mathrm{T}} \mathbf{M} - \boldsymbol{\mu}_{\ddot{\boldsymbol{\Phi}}}^{\mathrm{T}} \bar{\mathbf{P}} \right) \right\} \hat{\ddot{\mathbf{q}}}' \\
- \left\{ \boldsymbol{\mu}_2^{\mathrm{T}} \boldsymbol{\Phi}_{\mathbf{q}}^{\mathrm{T}} \right\} \boldsymbol{\lambda}' \\
- \Bigg\{ \left(\boldsymbol{\mu}^{\mathrm{T}} \left(\mathbf{Q}_{\boldsymbol{\rho}} - \mathbf{M}_{\boldsymbol{\rho}} \ddot{\mathbf{q}}^* - \boldsymbol{\Phi}_{\mathbf{q}\boldsymbol{\rho}}^{\mathrm{T}} \left(\boldsymbol{\lambda}^* + \boldsymbol{\alpha} \boldsymbol{\Phi} \right) - \boldsymbol{\Phi}_{\mathbf{q}}^{\mathrm{T}} \boldsymbol{\alpha} \boldsymbol{\Phi}_{\boldsymbol{\rho}} \right) - \boldsymbol{\mu}_{\boldsymbol{\Phi}}^{\mathrm{T}} \boldsymbol{\Phi}_{\boldsymbol{\rho}} \right. \\
- \boldsymbol{\mu}_{\dot{\boldsymbol{\Phi}}}^{\mathrm{T}} \left(\boldsymbol{\Phi}_{\mathbf{q}\boldsymbol{\rho}}^{\mathrm{T}} \varsigma \boldsymbol{\alpha} \dot{\boldsymbol{\Phi}} - \bar{\mathbf{P}}_{\boldsymbol{\rho}} \left(\dot{\mathbf{q}}^* - \dot{\mathbf{q}} \right) + \boldsymbol{\Phi}_{\mathbf{q}}^{\mathrm{T}} \varsigma \boldsymbol{\alpha} \dot{\boldsymbol{\Phi}}_{\boldsymbol{\rho}} \right) \\
\left. - \boldsymbol{\mu}_{\ddot{\boldsymbol{\Phi}}}^{\mathrm{T}} \left(\boldsymbol{\Phi}_{\mathbf{q}\boldsymbol{\rho}}^{\mathrm{T}} \varsigma \boldsymbol{\alpha} \ddot{\boldsymbol{\Phi}} - \bar{\mathbf{P}}_{\boldsymbol{\rho}} \left(\ddot{\mathbf{q}}^* - \ddot{\mathbf{q}} \right) + \boldsymbol{\Phi}_{\mathbf{q}}^{\mathrm{T}} \varsigma \boldsymbol{\alpha} \ddot{\boldsymbol{\Phi}}_{\boldsymbol{\rho}} \right) \right) \Bigg\}
\end{aligned} \tag{23}
$$

in which all magnitudes are evaluated at time t_i.

The adjoint Lagrangian can be defined using the previous instant Lagrangian (22) and the discrete integral equations (15):

$$
\mathscr{L} = \frac{h}{2} \left(\mathscr{L}_0 + \mathscr{L}_n \right) + h \sum_{i=1}^{n-1} \mathscr{L}_i \tag{24}
$$

where, once again, h is the time step of the discretization, $n = \frac{t_F - t_0}{h}$ the number of steps and $\mathscr{L}_i$ the value of $\mathscr{L}$ at the time $ih + t_0$.

Analogously, the gradient of the Lagrangian involving a discrete integral can be computed as:

$$
\mathscr{L}' = \frac{h}{2} \left(\mathscr{L}_0' + \mathscr{L}_n' \right) + h \sum_{i=1}^{n-1} \mathscr{L}_i' \tag{25}
$$

Once defined the integration rule, the instant Lagrangian sensitivities can be substituted into (25), conforming a unique expression with the adjoint variables, the sensitivities of the states and the sensitivities of the Lagrange multipliers as unknowns. Since the value of the Lagrangian and its gradient are equal to the cost function and its gradient, respectively, for any value of the adjoint variables, these adjoint variables can be selected such as they nullify the terms multiplying the unknown sensitivities of the states and the Lagrange multipliers, hence avoiding their calculation.

Returning again to equation (23), it can be seen that $\hat{\dot{\mathbf{q}}}'$ and $\hat{\ddot{\mathbf{q}}}'$ could be transformed into expressions dependent on the sensitivities of the previous step of time t_{i-1} using (4). Therefore, the instant gradient of the Lagrangian for any time t_i is:

$$
\begin{aligned}
\mathscr{L}_i' = \boldsymbol{\psi}' - \Bigg\{ & \boldsymbol{\mu}^{\mathrm{T}} \left(\frac{1}{\beta h^2}\mathbf{M} + \frac{\gamma}{\beta h}\bar{\mathbf{C}} + \bar{\mathbf{K}} \right) \\
& + \boldsymbol{\mu}_{\dot{\boldsymbol{\Phi}}}^{\mathrm{T}} \left(-\bar{\mathbf{P}}\frac{\gamma}{\beta h} - \bar{\mathbf{P}}_{\mathbf{q}} \left(\dot{\mathbf{q}}^* - \dot{\mathbf{q}}\right) + \boldsymbol{\Phi}_{\mathbf{qq}}^{\mathrm{T}} \varsigma \boldsymbol{\alpha} \dot{\boldsymbol{\Phi}} + \boldsymbol{\Phi}_{\mathbf{q}}^{\mathrm{T}} \varsigma \boldsymbol{\alpha} \left(\boldsymbol{\Phi}_{\mathbf{qq}} \dot{\mathbf{q}} + \boldsymbol{\Phi}_{\mathbf{q}t} \right) \right) \\
& + \boldsymbol{\mu}_{\ddot{\boldsymbol{\Phi}}}^{\mathrm{T}} \left(-\bar{\mathbf{P}}\frac{1}{\beta h^2} - \bar{\mathbf{P}}_{\mathbf{q}} \left(\ddot{\mathbf{q}}^* - \ddot{\mathbf{q}}\right) + \boldsymbol{\Phi}_{\mathbf{qq}}^{\mathrm{T}} \varsigma \boldsymbol{\alpha} \ddot{\boldsymbol{\Phi}} + \boldsymbol{\Phi}_{\mathbf{q}}^{\mathrm{T}} \varsigma \boldsymbol{\alpha} \left(\boldsymbol{\Phi}_{\mathbf{qq}} \ddot{\mathbf{q}} + \dot{\boldsymbol{\Phi}}_{\mathbf{qq}} \dot{\mathbf{q}} + \dot{\boldsymbol{\Phi}}_{\mathbf{q}t} \right) \right) + \boldsymbol{\mu}_{\boldsymbol{\Phi}}^{\mathrm{T}} \boldsymbol{\Phi}_{\mathbf{q}} \Bigg\} \mathbf{q}' \\
& - \left\{ \boldsymbol{\mu}_{\dot{\boldsymbol{\Phi}}}^{\mathrm{T}} \left(\bar{\mathbf{P}} + \varsigma \boldsymbol{\Phi}_{\mathbf{q}}^{\mathrm{T}} \boldsymbol{\alpha} \boldsymbol{\Phi}_{\mathbf{q}} \right) + \boldsymbol{\mu}_{\ddot{\boldsymbol{\Phi}}}^{\mathrm{T}} \left(\boldsymbol{\Phi}_{\mathbf{q}}^{\mathrm{T}} \varsigma \boldsymbol{\alpha} \left(\boldsymbol{\Phi}_{\mathbf{qq}} \dot{\mathbf{q}} + \dot{\boldsymbol{\Phi}}_{\mathbf{q}} + \boldsymbol{\Phi}_{\mathbf{q}t} \right) \right) \right\} \dot{\mathbf{q}}' \\
& - \left\{ \boldsymbol{\mu}_{\ddot{\boldsymbol{\Phi}}}^{\mathrm{T}} \left(\bar{\mathbf{P}} + \varsigma \boldsymbol{\Phi}_{\mathbf{q}}^{\mathrm{T}} \boldsymbol{\alpha} \boldsymbol{\Phi}_{\mathbf{q}} \right) \right\} \ddot{\mathbf{q}}' \\
& - \left\{ \left(\boldsymbol{\mu}^{\mathrm{T}} \mathbf{C} - \boldsymbol{\mu}_{\dot{\boldsymbol{\Phi}}}^{\mathrm{T}} \bar{\mathbf{P}} \right) \right\} \left\{ -\frac{\gamma}{\beta h} \mathbf{q}_{i-1}' - \left(\frac{\gamma}{\beta} - 1 \right) \dot{\mathbf{q}}_{i-1}' - \left(\frac{\gamma}{2\beta} - 1 \right) h \ddot{\mathbf{q}}_{i-1}' \right\} \\
& - \left\{ \left(\boldsymbol{\mu}^{\mathrm{T}} \mathbf{M} - \boldsymbol{\mu}_{\ddot{\boldsymbol{\Phi}}}^{\mathrm{T}} \bar{\mathbf{P}} \right) \right\} \left\{ -\frac{1}{\beta h^2} \mathbf{q}_{i-1} - \frac{1}{\beta h} \dot{\mathbf{q}}_{i-1} - \left(\frac{1}{2\beta} - 1 \right) \ddot{\mathbf{q}}_{i-1} \right\} \\
& - \left\{ \boldsymbol{\mu}_2^{\mathrm{T}} \boldsymbol{\Phi}_{\mathbf{q}}^{\mathrm{T}} \right\} \boldsymbol{\lambda}' \\
& - \Bigg\{ \left(\boldsymbol{\mu}^{\mathrm{T}} \left(\mathbf{Q}_{\boldsymbol{\rho}} - \mathbf{M}_{\boldsymbol{\rho}} \ddot{\mathbf{q}}^* - \boldsymbol{\Phi}_{\mathbf{q}\boldsymbol{\rho}}^{\mathrm{T}} \left(\boldsymbol{\lambda}^* + \boldsymbol{\alpha} \boldsymbol{\Phi} \right) - \boldsymbol{\Phi}_{\mathbf{q}}^{\mathrm{T}} \boldsymbol{\alpha} \boldsymbol{\Phi}_{\boldsymbol{\rho}} \right) - \boldsymbol{\mu}_{\boldsymbol{\Phi}}^{\mathrm{T}} \boldsymbol{\Phi}_{\boldsymbol{\rho}} \right. \\
& \quad - \boldsymbol{\mu}_{\dot{\boldsymbol{\Phi}}}^{\mathrm{T}} \left(\boldsymbol{\Phi}_{\mathbf{q}\boldsymbol{\rho}}^{\mathrm{T}} \varsigma \boldsymbol{\alpha} \dot{\boldsymbol{\Phi}} - \bar{\mathbf{P}}_{\boldsymbol{\rho}} \left(\dot{\mathbf{q}}^* - \dot{\mathbf{q}} \right) + \boldsymbol{\Phi}_{\mathbf{q}}^{\mathrm{T}} \varsigma \boldsymbol{\alpha} \dot{\boldsymbol{\Phi}}_{\boldsymbol{\rho}} \right) \\
& \quad \left. - \boldsymbol{\mu}_{\ddot{\boldsymbol{\Phi}}}^{\mathrm{T}} \left(\boldsymbol{\Phi}_{\mathbf{q}\boldsymbol{\rho}}^{\mathrm{T}} \varsigma \boldsymbol{\alpha} \ddot{\boldsymbol{\Phi}} - \bar{\mathbf{P}}_{\boldsymbol{\rho}} \left(\ddot{\mathbf{q}}^* - \ddot{\mathbf{q}} \right) + \boldsymbol{\Phi}_{\mathbf{q}}^{\mathrm{T}} \varsigma \boldsymbol{\alpha} \ddot{\boldsymbol{\Phi}}_{\boldsymbol{\rho}} \right) \right) \Bigg\}
\end{aligned}
\tag{26}
$$

in which the subscript i indicating magnitudes evaluated at time t_i is eliminated for the sake of clearness.

Observe that the sensitivity of each instant Lagrangian involves the sensitivities of the states in the time step t_i and in the previous one t_{i-1}. Therefore, the instant Lagrangians at consecutive time steps have to be calculated jointly in order to nullify the terms multiplying the sensitivity of a state in a given step of time. The relation among instant expressions has to be done following the scheme of integration (25) paying special attention to the coefficients multiplying each Lagrangian.

Let us now consider two subsequent time steps t_i and t_{i+1}, none of them being the initial or final time of the dynamic simulation. The expressions of the instant gradient of the Lagrangian will appear in (25) multiplied by the same coefficient h, so they could be simply added scaled by this coefficient. The result of this sum will deliver a set of terms multiplying the sensitivities of the states and Lagrange multipliers at t_i, and others at t_{i+1}. Observe that, since the sensitivities of the states are integrated forward in time, the sensitivities at t_i only affect the instant gradient of the Lagrangian at t_i and t_{i+1}. This sum (omitted here for the sake of clearness and brevity) supplies the terms that multiply the sensitivities of the states at t_i, and thus, the ones that have to be nullified in order to avoid these state sensitivities. Since no particular time has been chosen in this evaluation, the results are valid in the interval

(t_0, t_F). The set of equations resulting from this evaluation is:

$$\begin{aligned}\Bigg\{\boldsymbol{\mu}^{\mathrm{T}}\left(\frac{1}{\beta h^2}\mathbf{M}+\frac{\gamma}{\beta h}\bar{\mathbf{C}}+\bar{\mathbf{K}}\right)+\boldsymbol{\mu}_{\dot{\boldsymbol{\Phi}}}^{\mathrm{T}}\left(-\bar{\mathbf{P}}\frac{\gamma}{\beta h}-\bar{\mathbf{P}}_{\mathbf{q}}\left(\dot{\mathbf{q}}^{*}-\dot{\mathbf{q}}\right)+\boldsymbol{\Phi}_{\mathbf{qq}}^{\mathrm{T}}\varsigma\boldsymbol{\alpha}\dot{\boldsymbol{\Phi}}+\boldsymbol{\Phi}_{\mathbf{q}}^{\mathrm{T}}\varsigma\boldsymbol{\alpha}\dot{\boldsymbol{\Phi}}_{\mathbf{q}}\right)\\
+\boldsymbol{\mu}_{\ddot{\boldsymbol{\Phi}}}^{\mathrm{T}}\left(-\bar{\mathbf{P}}\frac{1}{\beta h^2}-\bar{\mathbf{P}}_{\mathbf{q}}\left(\ddot{\mathbf{q}}^{*}-\ddot{\mathbf{q}}\right)+\boldsymbol{\Phi}_{\mathbf{qq}}^{\mathrm{T}}\varsigma\boldsymbol{\alpha}\ddot{\boldsymbol{\Phi}}+\boldsymbol{\Phi}_{\mathbf{q}}^{\mathrm{T}}\varsigma\boldsymbol{\alpha}\ddot{\boldsymbol{\Phi}}_{\mathbf{q}}\right)+\boldsymbol{\mu}_{\boldsymbol{\Phi}}^{\mathrm{T}}\boldsymbol{\Phi}_{\mathbf{q}}\Bigg\}_{\{i\}}\\
+\left\{-\frac{\gamma}{\beta h}\mathbf{G}-\frac{1}{\beta h^2}\mathbf{H}\right\}_{\{i+1\}}=\mathbf{g}_{\mathbf{q}\{i\}}\end{aligned} \tag{27a}$$

$$\begin{aligned}\left\{\boldsymbol{\mu}_{\dot{\boldsymbol{\Phi}}}^{\mathrm{T}}\left(\bar{\mathbf{P}}+\varsigma\boldsymbol{\Phi}_{\mathbf{q}}^{\mathrm{T}}\boldsymbol{\alpha}\boldsymbol{\Phi}_{\mathbf{q}}\right)+\boldsymbol{\mu}_{\ddot{\boldsymbol{\Phi}}}^{\mathrm{T}}\left(\boldsymbol{\Phi}_{\mathbf{q}}^{\mathrm{T}}\varsigma\boldsymbol{\alpha}\left(2\dot{\boldsymbol{\Phi}}_{\mathbf{q}}\right)\right)\right\}_{\{i\}}\\
+\left\{\left(1-\frac{\gamma}{\beta}\right)\mathbf{G}-\frac{1}{\beta h}\mathbf{H}\right\}_{\{i+1\}}=\mathbf{g}_{\dot{\mathbf{q}}\{i\}}\end{aligned} \tag{27b}$$

$$\left\{\boldsymbol{\mu}_{\ddot{\boldsymbol{\Phi}}}^{\mathrm{T}}\left(\bar{\mathbf{P}}+\varsigma\boldsymbol{\Phi}_{\mathbf{q}}^{\mathrm{T}}\boldsymbol{\alpha}\boldsymbol{\Phi}_{\mathbf{q}}\right)\right\}_{\{i\}}+\left\{\left(1-\frac{\gamma}{2\beta}\right)h\mathbf{G}+\left(1-\frac{1}{2\beta}\right)\mathbf{H}\right\}_{\{i+1\}}=\mathbf{g}_{\ddot{\mathbf{q}}\{i\}} \tag{27c}$$

$$\left\{\boldsymbol{\mu}^{\mathrm{T}}\boldsymbol{\Phi}_{\mathbf{q}}^{\mathrm{T}}\right\}_{\{i\}}=\mathbf{g}_{\boldsymbol{\lambda}\{i\}} \tag{27d}$$

where:

$$\mathbf{G}=\boldsymbol{\mu}^{\mathrm{T}}\mathbf{C}-\boldsymbol{\mu}_{\dot{\boldsymbol{\Phi}}}^{\mathrm{T}}\bar{\mathbf{P}} \tag{28a}$$

$$\mathbf{H}=\boldsymbol{\mu}^{\mathrm{T}}\mathbf{M}-\boldsymbol{\mu}_{\ddot{\boldsymbol{\Phi}}}^{\mathrm{T}}\bar{\mathbf{P}} \tag{28b}$$

These equations can be solved sequentially: first, $\boldsymbol{\mu}_{\ddot{\boldsymbol{\Phi}}}$ can be determined from (27c); second, the value of $\boldsymbol{\mu}_{\ddot{\boldsymbol{\Phi}}}$ can be substituted in (27b), so $\boldsymbol{\mu}_{\dot{\boldsymbol{\Phi}}}$ can be obtained; third and last, (27a) and (27d) can be combined and solved jointly, giving as result the values of $\boldsymbol{\mu}$ and $\boldsymbol{\mu}_{\boldsymbol{\Phi}}$. The solution of this third system of equations is equivalent to the one solved in [21] for the continuous approach, and suffers the same problems of indetermination when redundant constraints are part of the multibody model. Following the algorithm proposed in [21], this system can be solved using an augmented Lagrange scheme with (27a) scaled by a factor of βh^2 to improve its numerical conditioning. The final expressions are:

$$\left(\mathbf{M}^{d}+\gamma h\bar{\mathbf{C}}+\beta h^2\bar{\mathbf{K}}\right)^{\mathrm{T}}\boldsymbol{\mu}+\beta h^2\boldsymbol{\Phi}_{\mathbf{q}}^{\mathrm{T}}\left(\boldsymbol{\mu}_{\boldsymbol{\Phi}}^{*(i)}-\boldsymbol{\alpha}_a\left(\mathbf{g}_{\boldsymbol{\lambda}}-\boldsymbol{\Phi}_{\mathbf{q}}\boldsymbol{\mu}\right)\right)=\mathbf{r}_1 \tag{29a}$$

$$\boldsymbol{\mu}_{\boldsymbol{\Phi}}^{*(i)}=\boldsymbol{\mu}_{\boldsymbol{\Phi}}^{*(i-1)}-\boldsymbol{\alpha}_a\left(\mathbf{g}_{\boldsymbol{\lambda}}-\boldsymbol{\Phi}_{\mathbf{q}}\boldsymbol{\mu}\right) \tag{29b}$$

with

$$\begin{aligned}\mathbf{r}_1=\beta h^2\Bigg\{\mathbf{g}_{\mathbf{q}}-\boldsymbol{\mu}_{\dot{\boldsymbol{\Phi}}}^{\mathrm{T}}\left(-\bar{\mathbf{P}}\frac{\gamma}{\beta h}-\bar{\mathbf{P}}_{\mathbf{q}}\left(\dot{\mathbf{q}}^{*}-\dot{\mathbf{q}}\right)+\boldsymbol{\Phi}_{\mathbf{qq}}^{\mathrm{T}}\varsigma\boldsymbol{\alpha}\dot{\boldsymbol{\Phi}}+\boldsymbol{\Phi}_{\mathbf{q}}^{\mathrm{T}}\varsigma\boldsymbol{\alpha}\left(\boldsymbol{\Phi}_{\mathbf{qq}}\dot{\mathbf{q}}+\boldsymbol{\Phi}_{\mathbf{q}t}\right)\right)\\
+\boldsymbol{\mu}_{\ddot{\boldsymbol{\Phi}}}^{\mathrm{T}}\left(-\bar{\mathbf{P}}\frac{1}{\beta h^2}-\bar{\mathbf{P}}_{\mathbf{q}}\left(\ddot{\mathbf{q}}^{*}-\ddot{\mathbf{q}}\right)+\boldsymbol{\Phi}_{\mathbf{qq}}^{\mathrm{T}}\varsigma\boldsymbol{\alpha}\ddot{\boldsymbol{\Phi}}+\boldsymbol{\Phi}_{\mathbf{q}}^{\mathrm{T}}\varsigma\boldsymbol{\alpha}\left(\boldsymbol{\Phi}_{\mathbf{qq}}\ddot{\mathbf{q}}+\dot{\boldsymbol{\Phi}}_{\mathbf{qq}}\dot{\mathbf{q}}+\dot{\boldsymbol{\Phi}}_{\mathbf{q}t}\right)\right)\Bigg\}_{\{i\}}\\
-\left\{-\frac{\gamma}{\beta h}\mathbf{G}-\frac{1}{\beta h^2}\mathbf{H}\right\}_{\{i+1\}}\end{aligned} \tag{30}$$

In the discrete adjoint problem, the different expressions used to solve the initial position, velocity and acceleration problems have to be considered in the Lagrangian in order to incorporate their effect on the sensitivities. Consequently, the adjoint of the initial position and velocity problem have to be computed at t_0, but also the adjoint of the initial dynamic acceleration problem have to be addressed. In this work, the initial acceleration problem is solved by means of the penalty approach described in [27].

The initial positions of the dependent coordinates $\mathbf{q}_0$ are obtained by means of the kinematic initial position problem, in which a kinematic model is enforced to fulfill a set of constraints $\mathbf{\Phi}$ for a given set of values of its degrees of freedom (dof) $\mathbf{z} \in \mathbb{R}^d$, being d the number of dof. This problem is commonly solved using a Newton-Raphson scheme with the form:

$$\begin{bmatrix} \mathbf{\Phi_q} \\ \mathbf{B} \end{bmatrix} \Delta \mathbf{q} = \begin{bmatrix} -\mathbf{\Phi} \\ \mathbf{0} \end{bmatrix} \tag{31}$$

in which $\mathbf{B} \in \mathbb{R}^{d \times n}$ is a constant matrix composed by "1"s and "0"s such that:

$$\mathbf{Bq} = \mathbf{z} \tag{32}$$

This formalism can be extended to non constant $\mathbf{B}$ matrices, i. e. to problems where the degrees of freedom are not included in the vector of dependent coordinates $\mathbf{q}_0$. Nevertheless, only constant $\mathbf{B}$ matrices will be considered here.

The velocity problem is described by a similar set of linear equations:

$$\begin{bmatrix} \mathbf{\Phi_q} \\ \mathbf{B} \end{bmatrix} \dot{\mathbf{q}} = \begin{bmatrix} -\mathbf{\Phi}_t \\ \dot{\mathbf{z}} \end{bmatrix} \tag{33}$$

The implicit Newmark numerical integrator requires initial accelerations to compute the positions, velocities and accelerations at the following instant of time. These accelerations can be computed with multiple formulations, such as an index-1 DAE, a matrix R formulation or the penalty approach described in [27]. With any of the previous problems, the dependent positions and velocities computed with the initial position and velocity problems can be used to build the system of dynamic equations, and any of them can be solved with the accelerations as main variables. As it was mentioned above, the penalty approach will be the method considered hereinafter.

The penalty formulation proposed by Bayo et al. [27] presents a solution for the equations of motion by substituting the Lagrange multipliers of the classical Lagrange's formulation by a penalized term composed by the constraints vector in positions, velocities and accelerations, which transforms the original DAE into and ODE with the form:

$$\mathbf{M}\ddot{\mathbf{q}} + \mathbf{\Phi_q}^{\mathrm{T}} \boldsymbol{\alpha} \left(\ddot{\mathbf{\Phi}} + 2\boldsymbol{\Omega}\boldsymbol{\xi}\dot{\mathbf{\Phi}} + \boldsymbol{\Omega}^2 \mathbf{\Phi} \right) = \mathbf{Q} \tag{34}$$

Unlike the notation presented in [27], here the penalizer originally denoted as $\boldsymbol{\mu}$ is renamed as $\boldsymbol{\xi}$ in order to eliminate possible misunderstandings with the set of adjoint variables described in the in the following lines. The application of this formulation to an initial acceleration problem transforms the ODE into a set of linear equations, since positions and velocities are already determined by the correspondent kinematic problems.

Equation (34) can be reformulated to simplify the notation as:

$$\bar{\mathbf{M}}\ddot{\mathbf{z}} = \bar{\mathbf{Q}} \tag{35}$$

in which:

$$\bar{\mathbf{M}} = \mathbf{M} + \mathbf{\Phi_q}^{\mathrm{T}} \boldsymbol{\alpha} \mathbf{\Phi_q} \tag{36a}$$

$$\bar{\mathbf{Q}} = \mathbf{Q} - \mathbf{\Phi_q}^{\mathrm{T}} \boldsymbol{\alpha} \left(\dot{\mathbf{\Phi}}_\mathbf{q} \dot{\mathbf{q}} + \dot{\mathbf{\Phi}}_t + 2\boldsymbol{\Omega}\boldsymbol{\xi}\dot{\mathbf{\Phi}} + \boldsymbol{\Omega}^2 \mathbf{\Phi} \right) \tag{36b}$$

where the leading matrix of the system $\bar{\mathbf{M}}$ is symmetric and always has inverse.

Once described the initial position, velocity and acceleration problems, derivatives can be taken to obtain their correspondent sensitivity equations. Considering (31), the sensitivities of $\mathbf{q}$ can be reached by means of:

$$\begin{bmatrix} \boldsymbol{\Phi}_{\mathbf{q}} \\ \mathbf{B} \end{bmatrix} \mathbf{q}' = \begin{bmatrix} -\boldsymbol{\Phi}_{\boldsymbol{\rho}} \\ \mathbf{z}' \end{bmatrix} \tag{37}$$

Deriving (33), the sensitivities of the velocities of the states are directly obtained with:

$$\begin{bmatrix} \boldsymbol{\Phi}_{\mathbf{q}} \\ \mathbf{B} \end{bmatrix} \dot{\mathbf{q}}' = \begin{bmatrix} -\dot{\boldsymbol{\Phi}}_{\mathbf{q}}\mathbf{q}' - \dot{\boldsymbol{\Phi}}_{\boldsymbol{\rho}} \\ \dot{\mathbf{z}}' \end{bmatrix} \tag{38}$$

The derivation of the dynamic penalty problem, already studied by Pagalday in [28], yields:

$$\bar{\mathbf{M}}\ddot{\mathbf{q}}' + \bar{\mathbf{C}}\dot{\mathbf{q}}' + \left(\bar{\mathbf{M}}_{\mathbf{q}}\ddot{\mathbf{q}} + \bar{\mathbf{K}}\right)\mathbf{q}' = \bar{\mathbf{Q}}^{\boldsymbol{\rho}} - \bar{\mathbf{M}}^{\boldsymbol{\rho}}\ddot{\mathbf{q}} \tag{39}$$

where:

$$\bar{\mathbf{M}}_{\mathbf{q}} = \mathbf{M}_{\mathbf{q}} + \boldsymbol{\Phi}_{\mathbf{qq}}^{\mathrm{T}}\boldsymbol{\alpha}\boldsymbol{\Phi}_{\mathbf{q}} + \boldsymbol{\Phi}_{\mathbf{q}}^{\mathrm{T}}\boldsymbol{\alpha}\boldsymbol{\Phi}_{\mathbf{qq}} \tag{40a}$$

$$\bar{\mathbf{M}}^{\boldsymbol{\rho}} = \mathbf{M}_{\boldsymbol{\rho}} + \boldsymbol{\Phi}_{\mathbf{q}\boldsymbol{\rho}}^{\mathrm{T}}\boldsymbol{\alpha}\boldsymbol{\Phi}_{\mathbf{q}} + \boldsymbol{\Phi}_{\mathbf{q}}^{\mathrm{T}}\boldsymbol{\alpha}\boldsymbol{\Phi}_{\mathbf{q}\boldsymbol{\rho}} \tag{40b}$$

$$\begin{aligned} \bar{\mathbf{K}} = -\bar{\mathbf{Q}}_{\mathbf{q}} = \mathbf{K} + \boldsymbol{\Phi}_{\mathbf{qq}}^{\mathrm{T}} &\left(\dot{\boldsymbol{\Phi}}_{\mathbf{q}}\dot{\mathbf{q}} + \dot{\boldsymbol{\Phi}}_{t} + 2\boldsymbol{\Omega}\boldsymbol{\xi}\dot{\boldsymbol{\Phi}} + \boldsymbol{\Omega}^2\boldsymbol{\Phi}\right) \\ +\boldsymbol{\Phi}_{\mathbf{q}}^{\mathrm{T}} &\left(\dot{\boldsymbol{\Phi}}_{\mathbf{qq}}\dot{\mathbf{q}} + \dot{\boldsymbol{\Phi}}_{t\mathbf{q}} + 2\boldsymbol{\Omega}\boldsymbol{\xi}\dot{\boldsymbol{\Phi}}_{\mathbf{q}} + \boldsymbol{\Omega}^2\boldsymbol{\Phi}_{\mathbf{q}}\right) \end{aligned} \tag{40c}$$

$$\bar{\mathbf{C}} = -\bar{\mathbf{Q}}_{\dot{\mathbf{q}}} = \mathbf{C} + \boldsymbol{\Phi}_{\mathbf{q}}^{\mathrm{T}}\left(\dot{\boldsymbol{\Phi}}_{\mathbf{q}\dot{\mathbf{q}}}\dot{\mathbf{q}} + \dot{\boldsymbol{\Phi}}_{\mathbf{q}} + \dot{\boldsymbol{\Phi}}_{t\dot{\mathbf{q}}} + 2\boldsymbol{\Omega}\boldsymbol{\xi}\dot{\boldsymbol{\Phi}}_{\dot{\mathbf{q}}}\right) = \mathbf{C} + \boldsymbol{\Phi}_{\mathbf{q}}^{\mathrm{T}}\left(2\dot{\boldsymbol{\Phi}}_{\mathbf{q}} + 2\boldsymbol{\Omega}\boldsymbol{\xi}\dot{\boldsymbol{\Phi}}_{\dot{\mathbf{q}}}\right) \tag{40d}$$

$$\bar{\mathbf{Q}}^{\boldsymbol{\rho}} = \mathbf{Q}_{\boldsymbol{\rho}} - \boldsymbol{\Phi}_{\mathbf{q}\boldsymbol{\rho}}^{\mathrm{T}}\boldsymbol{\alpha}\left(\dot{\boldsymbol{\Phi}}_{\mathbf{q}}\dot{\mathbf{q}} + \dot{\boldsymbol{\Phi}}_{t} + 2\boldsymbol{\Omega}\boldsymbol{\xi}\dot{\boldsymbol{\Phi}} + \boldsymbol{\Omega}^2\boldsymbol{\Phi}\right) - \boldsymbol{\Phi}_{\mathbf{q}}^{\mathrm{T}}\boldsymbol{\alpha}\left(\dot{\boldsymbol{\Phi}}_{\mathbf{q}\boldsymbol{\rho}}\dot{\mathbf{q}} + \dot{\boldsymbol{\Phi}}_{t\mathbf{q}} + 2\boldsymbol{\Omega}\boldsymbol{\xi}\dot{\boldsymbol{\Phi}}_{\boldsymbol{\rho}} + \boldsymbol{\Omega}^2\boldsymbol{\Phi}_{\boldsymbol{\rho}}\right) \tag{40e}$$

Observe that neither the kinematic problems in positions and velocities neither the penalty acceleration problem depend on any previous value, hence the integrator does not have to be applied to these expressions.

Equations (31), (33) and (35) allow the computation of the instant Lagrangian at the initial time t_0 as:

$$\begin{aligned} \mathscr{L}_0 = \boldsymbol{\psi}_0 - \boldsymbol{\mu}_{\boldsymbol{\Phi}0}^{\mathrm{T}}\left(\begin{bmatrix} \boldsymbol{\Phi} \\ \mathbf{Bq} - \mathbf{z} \end{bmatrix}\right) - \boldsymbol{\mu}_{\dot{\boldsymbol{\Phi}}0}^{\mathrm{T}}\left(\begin{bmatrix} \boldsymbol{\Phi}_{\mathbf{q}} \\ \mathbf{B} \end{bmatrix}\dot{\mathbf{q}} + \begin{bmatrix} \boldsymbol{\Phi}_{t} \\ -\dot{\mathbf{z}} \end{bmatrix}\right) - \\ -\boldsymbol{\mu}_0^{\mathrm{T}}\left(\bar{\mathbf{M}}\ddot{\mathbf{q}} - \bar{\mathbf{Q}}\right) \end{aligned} \tag{41}$$

Now, applying the sensitivity expressions (37), (38) and (39) of the initial problems, the gradient of the instant Lagrangian at the initial time step is:

$$\begin{aligned} \mathscr{L}_0' = \boldsymbol{\psi}_0' - \boldsymbol{\mu}_{\boldsymbol{\Phi}0}^{\mathrm{T}}\left(\begin{bmatrix} \boldsymbol{\Phi}_{\mathbf{q}} \\ \mathbf{B} \end{bmatrix}\mathbf{q}' - \begin{bmatrix} -\boldsymbol{\Phi}_{\boldsymbol{\rho}} \\ \mathbf{z}' \end{bmatrix}\right) - \boldsymbol{\mu}_{\dot{\boldsymbol{\Phi}}0}^{\mathrm{T}}\left(\begin{bmatrix} \boldsymbol{\Phi}_{\mathbf{q}} \\ \mathbf{B} \end{bmatrix}\dot{\mathbf{q}}' + \begin{bmatrix} \dot{\boldsymbol{\Phi}}_{\mathbf{q}} \\ \mathbf{0} \end{bmatrix}\mathbf{q}' + \begin{bmatrix} \dot{\boldsymbol{\Phi}}_{\boldsymbol{\rho}} \\ -\dot{\mathbf{z}}' \end{bmatrix}\right) - \\ -\boldsymbol{\mu}_0^{\mathrm{T}}\left(\bar{\mathbf{M}}\ddot{\mathbf{q}}' + \bar{\mathbf{C}}\dot{\mathbf{q}}' + \left(\bar{\mathbf{M}}_{\mathbf{q}}\ddot{\mathbf{q}} + \bar{\mathbf{K}}\right)\mathbf{q}' - \bar{\mathbf{Q}}_{\boldsymbol{\rho}} + \bar{\mathbf{M}}_{\boldsymbol{\rho}}\ddot{\mathbf{q}}\right) \end{aligned} \tag{42}$$

In the two previous equations, $\boldsymbol{\mu}_{\boldsymbol{\Phi}0} \in \mathbb{R}^{(m+d)\times o}$ is the adjoint variable related to the initial position equations, $\boldsymbol{\mu}_{\dot{\boldsymbol{\Phi}}0} \in \mathbb{R}^{(m+d)\times o}$ is the variable related to the fulfillment of the initial velocity problem and $\boldsymbol{\mu}_0 \in \mathbb{R}^{n\times o}$ is related to the compliment of the dynamic penalty problem, where m is the number of constraints, d the number of degrees of freedom, n the quantity of dependent coordinates and o the number of objective functions.

In (42), there are no unprojected velocities or accelerations, neither Lagrange multipliers, but there are 3 sets of unknown sensitivities: $\mathbf{z}'$, $\dot{\mathbf{z}}'$ and $\ddot{\mathbf{z}}'$. Considering the integration step between t_0 and t_1 of the Lagrangian gradient using (42), (26) and the coefficients of the trapezoidal rule (25), a set of expressions multiplying the unknown sensitivities can be identified. The following system of adjoint equations at the initial time t_0 can obtained nullifying these expressions:

$$\left\{\boldsymbol{\mu}_0^{\mathrm{T}}\left(\bar{\mathbf{M}}_{\mathbf{q}}\ddot{\mathbf{q}}+\bar{\mathbf{K}}\right)+\boldsymbol{\mu}_{\boldsymbol{\Phi}0}^{\mathrm{T}}\left(\begin{bmatrix}\boldsymbol{\Phi}_{\mathbf{q}}\\ \mathbf{B}\end{bmatrix}\right)+\boldsymbol{\mu}_{\dot{\boldsymbol{\Phi}}}^{\mathrm{T}}\left(\begin{bmatrix}\dot{\boldsymbol{\Phi}}_{\mathbf{q}}\\ \mathbf{0}\end{bmatrix}\right)\right\}_{\{t_0\}}+2\left\{-\frac{\gamma}{\beta h}\mathbf{G}-\frac{1}{\beta h^2}\mathbf{H}\right\}_{\{t_0+h\}}=\mathbf{g}_{\mathbf{q}\{t_0\}} \tag{43a}$$

$$\left\{\boldsymbol{\mu}_0^{\mathrm{T}}\left(\bar{\mathbf{C}}\right)+\boldsymbol{\mu}_{\dot{\boldsymbol{\Phi}}0}^{\mathrm{T}}\left(\begin{bmatrix}\boldsymbol{\Phi}_{\mathbf{q}}\\ \mathbf{B}\end{bmatrix}\right)\right\}_{\{t_0\}}+2\left\{\left(1-\frac{\gamma}{\beta}\right)\mathbf{G}+\left(-\frac{1}{\beta h}\right)\mathbf{H}\right\}_{\{t_0+h\}}=\mathbf{g}_{\dot{\mathbf{q}}\{t_0\}} \tag{43b}$$

$$\left\{\boldsymbol{\mu}_0^{\mathrm{T}}\left(\bar{\mathbf{M}}\right)\right\}_{\{t_0\}}+2\left\{\left(1-\frac{\gamma}{2\beta}\right)h\mathbf{G}+\left(1-\frac{1}{2\beta}\right)\mathbf{H}\right\}_{\{t_0+h\}}=\mathbf{g}_{\ddot{\mathbf{q}}\{t_0\}} \tag{43c}$$

Observe that a coefficient 2 appears now multiplying the accumulated terms $\mathbf{G}$ and $\mathbf{H}$ due to the integration scheme used (25). Looking at this equation, the Lagrangian at t_0 is multiplied by $h/2$, while the next time step t_1 is multiplied by h. This coefficient arise during the addition of equations and the nullifying of the terms related to the sensitivities of the states at t_0. It should be remarked that this coefficient is exclusively valid for the rule of integration (25). If a different scheme of integration is used, different values of this constant will come out.

The system of equations (43) can be easily solved sequentially: firstly, $\boldsymbol{\mu}_0$ can be determined from (43c) (this system is compatible determined, hence it has a unique solution); secondly, $\boldsymbol{\mu}_{\dot{\boldsymbol{\Phi}}0}$ can be obtained from (43b). Thirdly, $\boldsymbol{\mu}_{\boldsymbol{\Phi}0}$ can be calculated from (43a).

It is important to note that the use of redundant constraints entails the existence of infinite valid solutions for $\boldsymbol{\mu}_{\dot{\boldsymbol{\Phi}}0}$, being one of them the minimum norm solution of the system. Since this system is solved only once per simulation, there is no need to use efficient techniques to solve it, so general routines of math libraries such as LAPACK could be employed. This minimum norm solution is considered and implemented in MBSLIM for the solution of both $\boldsymbol{\mu}_{\dot{\boldsymbol{\Phi}}0}$ and $\boldsymbol{\mu}_{\boldsymbol{\Phi}0}$.

Similarly to t_0, in t_F the effect of the integration rule have to be considered too. In the solution of the adjoint equations related to the sensitivities of the states and Lagrange multipliers at t_F-h, the accumulation terms $\mathbf{G}$ and $\mathbf{H}$ appear multiplied by a coefficient of 0.5 in (27).

Once solved the correspondent systems of adjoint equations at each time step, the gradient of the cost function can be computed with the remaining terms independently from the sensitivities of the states. The instant gradient for $t_i\in(t_0,t_F]$ can be computed as:

$$\begin{aligned}\boldsymbol{\psi}'_{t_i}=\mathbf{g}_{\boldsymbol{\rho}}+\boldsymbol{\mu}^{\mathrm{T}}&\left(\mathbf{Q}_{\boldsymbol{\rho}}-\mathbf{M}_{\boldsymbol{\rho}}\ddot{\mathbf{q}}^*-\boldsymbol{\Phi}_{\mathbf{q}\boldsymbol{\rho}}^{\mathrm{T}}\left(\boldsymbol{\lambda}^*+\boldsymbol{\alpha}\boldsymbol{\Phi}\right)-\boldsymbol{\Phi}_{\mathbf{q}}^{\mathrm{T}}\boldsymbol{\alpha}\boldsymbol{\Phi}_{\boldsymbol{\rho}}\right)\\ -\boldsymbol{\mu}_{\boldsymbol{\Phi}}^{\mathrm{T}}\boldsymbol{\Phi}_{\boldsymbol{\rho}}-\boldsymbol{\mu}_{\dot{\boldsymbol{\Phi}}}^{\mathrm{T}}&\left(\boldsymbol{\Phi}_{\mathbf{q}\boldsymbol{\rho}}^{\mathrm{T}}\varsigma\boldsymbol{\alpha}\dot{\boldsymbol{\Phi}}-\bar{\mathbf{P}}_{\boldsymbol{\rho}}\left(\dot{\mathbf{q}}^*-\dot{\mathbf{q}}\right)+\boldsymbol{\Phi}_{\mathbf{q}}^{\mathrm{T}}\varsigma\boldsymbol{\alpha}\dot{\boldsymbol{\Phi}}_{\boldsymbol{\rho}}\right)\\ -\boldsymbol{\mu}_{\ddot{\boldsymbol{\Phi}}}^{\mathrm{T}}&\left(\boldsymbol{\Phi}_{\mathbf{q}\boldsymbol{\rho}}^{\mathrm{T}}\varsigma\boldsymbol{\alpha}\ddot{\boldsymbol{\Phi}}-\bar{\mathbf{P}}_{\boldsymbol{\rho}}\left(\ddot{\mathbf{q}}^*-\ddot{\mathbf{q}}\right)+\boldsymbol{\Phi}_{\mathbf{q}}^{\mathrm{T}}\varsigma\boldsymbol{\alpha}\ddot{\boldsymbol{\Phi}}_{\boldsymbol{\rho}}\right)\end{aligned} \tag{44}$$

At t_0, the instant gradient of the cost function is:

$$\boldsymbol{\psi}'_{t_0} = \mathscr{L}'_{t_0} = \mathbf{g}_{\boldsymbol{\rho}} - \boldsymbol{\mu}^{\mathrm{T}}_{\boldsymbol{\Phi}0}\left(\begin{bmatrix}\boldsymbol{\Phi}_{\boldsymbol{\rho}} \\ -\mathbf{z}'\end{bmatrix}\right) - \boldsymbol{\mu}^{\mathrm{T}}_{\dot{\boldsymbol{\Phi}}0}\left(\begin{bmatrix}\dot{\boldsymbol{\Phi}}_{\boldsymbol{\rho}} \\ -\dot{\mathbf{z}}'\end{bmatrix}\right) - \boldsymbol{\mu}^{\mathrm{T}}_{0}\left(\bar{\mathbf{M}}^{\boldsymbol{\rho}}\ddot{\mathbf{q}} - \bar{\mathbf{Q}}^{\boldsymbol{\rho}}\right) \tag{45}$$

Applying the numerical integration (25), the gradient of the cost function can be obtained as:

$$\boldsymbol{\psi}' = \frac{h}{2}\left(\boldsymbol{\psi}'_0 + \boldsymbol{\psi}'_n\right) + h\sum_{i=1}^{n-1}\boldsymbol{\psi}'_i \tag{46}$$

The DAVM of the ALI3-P semi-recursive formulation can be generally computed by means of the following algorithm:

1. Solution of the dynamic problem and storage of the values of the states, the Lagrange multipliers and the projected and unprojected velocities and accelerations at each time step.
2. Initiation of the backwards computation of the adjoint variable sensitivity at t_F with the accumulation terms $\mathbf{G} = \mathbf{0}$ and $\mathbf{H} = \mathbf{0}$.
3. Determination of $\boldsymbol{\mu}_{\ddot{\boldsymbol{\Phi}}}$ from (27c).
4. Computation of $\boldsymbol{\mu}_{\dot{\boldsymbol{\Phi}}}$ from (27b).
5. Solution of $\boldsymbol{\mu}$ and $\boldsymbol{\mu}_{\boldsymbol{\Phi}}$ from (27a) and (27d).
6. Computation of the sensitivity of the instant Lagrangian (44) and integration in time by means of (46).
7. Computation of the accumulated terms $\mathbf{G}$ and $\mathbf{H}$ through (28) at the current time step.
8. Decrease of the time step and repetition of the stages from 2 to 6 until t_0 is reached.
9. At t_0, computation of $\boldsymbol{\mu}_0$ from (43c).
10. Calculation of $\boldsymbol{\mu}_{\dot{\boldsymbol{\Phi}}0}$ from (43b), using a minimum norm solver.
11. Determination of $\boldsymbol{\mu}_{\boldsymbol{\Phi}0}$ from (43a), using a minimum norm solver.
12. Computation of the sensitivity of the instant Lagrangian (42) and integration in time by means of (46).

Behold that most of the obstacles found in the CAVM applied to the ALI3-P formulation, such as time derivatives of mass and projection matrices, the application of a variable change, the addition of adjoint variables at t_F or the complex initialization process are avoided with this method. There is no additional derivatives apart from the ones present on the DDM, there is no need to include new adjoint variables for initialization purposes, and the initialization process is reduced to use the same expressions valid for instant of time $t_i \in (t_0, t_F]$ but with the accumulated terms equal to zero.

It should be remarked also that CAVM and DAVM yield very similar expressions, and equivalent computational times are expected.

6 Numerical experiments

In this section, the DAVM applied to ALI3-P formulations is tested with two multibody systems modeled with natural and relative coordinates. The relative coordinates semi-recursive formulations used are RTdyn0 ALI3-P and RTdyn1 ALI3-P, both presented in [16]. Results are compared with a reference response obtained with the matrix R formulation in natural coordinates described in [29] with 1 millisecond of time step. The sensitivity analyses have been executed with the multibody library MBSLIM on an Intel Core i7-8700 CPU at 3.20GHz running Windows 10 with Fortran Intel Parallel Studio XE 2018.

6.1 Five-bar mechanism

The five-bar mechanism used is a multibody system composed by 5 bars which has been traditionally used as benchmark problem to test sensitivity results [28, 30, 31, 5, 21] [5].

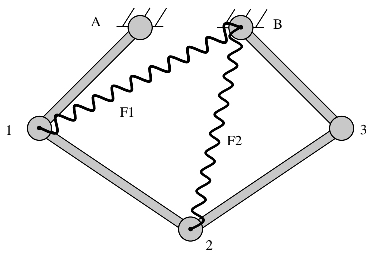

Fig. 1 Five-bar linkage.

The array objective function considered is:

$$\psi = \int_{t_F}^{t_0} \mathbf{g}\mathrm{dt} \tag{47}$$

with

$$\mathbf{g} = \begin{bmatrix} (\mathbf{r}_2 - \mathbf{r}_{20})^{\mathrm{T}} (\mathbf{r}_2 - \mathbf{r}_{20}) \\ \dot{\mathbf{r}}_2^{\mathrm{T}} \dot{\mathbf{r}}_2 \\ \ddot{\mathbf{r}}_2^{\mathrm{T}} \ddot{\mathbf{r}}_2 \end{bmatrix} \tag{48}$$

in which $\mathbf{r}_2$ is the position of the point identified as 2 in figure 1, whereas $\dot{\mathbf{r}}_2$ and $\ddot{\mathbf{r}}_2$ are its velocity and acceleration. The term $\mathbf{r}_{20}$ represents the position of point 2 at the initial instant of time $\mathbf{r}_{20} = \left[0.5\ -2.0\ 0.0\right]^{\mathrm{T}}$.

The mass, the length and the position of the center of mass of the bar A1 constitute the set of parameters of the system along with the natural lengths of the springs:

$$\boldsymbol{\rho} = \left[L_{s1}\ L_{s2}\ m_{A1}\ x_{A1}^{G}\ L_{A1}\right] \tag{49}$$

in which x_{A1}^{G} constitutes a simplified notation of $\left(\bar{\mathbf{r}}_{A1}^{G}\right)_x$.

The results of the sensitivity analysis for a 5 second maneuver of the mechanism subjected to gravitational and spring forces are displayed in table 1. Observe that the results are equivalent for both natural and relative coordinate models, which demonstrates that the method is valid for both constant or variable mass and projection matrices.

Harnessing the same mechanism, a second sensitivity problem is outlined. Let us consider that two actuators are connected to points A and B (see fig. 1), and they can introduce an angular force on the joints placed at this points. Behold that this is a 2-dof mechanism which can be completely determined by defining the values of two of the angles of its revolute joints[6]. An optimal control can be applied to this mechanism using these two angular forces as control inputs.

[5] The reader is referred to those works for a detailed description of the mechanism.

[6] This mechanism can have a direct and an inverted configuration for a given selection of dof, but the number of dof is still invariant.

	RTdyn0 ALI3-P	RTdyn1 ALI3-P	ALI3-P	Reference
$(\boldsymbol{\psi}^1)'_{L_{s1}}$	-4.228	-4.228	-4.228	-4.228
$(\boldsymbol{\psi}^1)'_{L_{s2}}$	3.212	3.212	3.212	3.212
$(\boldsymbol{\psi}^1)'_{m_{A1}}$	0.3186	0.3186	0.3186	0.3186
$(\boldsymbol{\psi}^1)'_{x^G_{A1}}$	0.4423	0.4423	0.4423	0.4423
$(\boldsymbol{\psi}^1)'_{L_{A1}}$	3.360	3.360	3.360	3.360
$(\boldsymbol{\psi}^2)'_{L_{s1}}$	-15.45	-15.45	-15.45	-15.45
$(\boldsymbol{\psi}^2)'_{L_{s2}}$	50.32	50.32	50.32	50.32
$(\boldsymbol{\psi}^2)'_{m_{A1}}$	0.9700	0.9700	0.9700	0.9700
$(\boldsymbol{\psi}^2)'_{x^G_{A1}}$	0.7454	0.7454	0.7454	0.7454
$(\boldsymbol{\psi}^2)'_{L_{A1}}$	-27.37	-27.37	-27.37	-27.37
$(\boldsymbol{\psi}^3)'_{L_{s1}}$	221.7	221.7	221.7	221.8
$(\boldsymbol{\psi}^3)'_{L_{s2}}$	2437	2437	2437	2437
$(\boldsymbol{\psi}^3)'_{m_{A1}}$	-32.51	-32.51	-32.51	-32.51
$(\boldsymbol{\psi}^3)'_{x^G_{A1}}$	-85.70	-85.70	-85.70	-85.70
$(\boldsymbol{\psi}^3)'_{L_{A1}}$	-2547	-2547	-2547	-2547

Table 1 Sensitivities of each component of objective function.

One approach to optimal control consists of the parameterization of these forces by means of splines, which allows a reduction in the number of parameters of the optimization problem. In this case, cyclic splines are employed [32].

The optimal control problem is omitted here since it is out of the scope of this paper, but the sensitivity analysis of the problem is studied for this application. The use of splines allow to easily increase the number of parameters, which makes possible to assess the effect of the size of the parameters vector on the total CPU time when a DAVM method is used.

Once guaranteed that the results are accurate with the first five-bar experiment, computational times with the force splines parameterized with 10, 25, 50, 100, 250 and 500 points each one are evaluated for DAVM and DDM methods applied to ALI3-P in natural and relative coordinates.

		Number of parameters					
		20	50	100	200	500	1000
DDM	ALI3-P	0.828	1.219	1.844	3.672	11.281	23.016
	RTdyn0 ALI3-P	0.672	0.734	0.844	1.109	1.828	3.109
	RTdyn1 ALI3-P	0.688	0.781	0.890	1.156	2.000	3.547
DAVM	ALI3-P	0.719	0.781	0.844	0.953	1.313	1.828
	RTdyn0 ALI3-P	0.672	0.688	0.781	0.844	1.188	1.688
	RTdyn1 ALI3-P	0.672	0.703	0.797	0.953	1.359	2.094

Table 2 CPU times (in seconds) for different numbers of sensitivity parameters.

Table 2 portraits the benefits of the DAVM with respect to the DDM in terms of computational time independently from the set of coordinates selected. CPU times of the reference response computed with matrix R formulation have been eliminated from table 2 since the goal of this table is to compare the performance of the differentiation methods within the same dynamic formulation.

6.2 Four-wheeled vehicle

The discrete sensitivity expressions are proved in a more complex real-life multibody model in order to test their validity, generality and performance. The mechanical system considered is the four-wheeled vehicle with articulated suspensions recently described in [16] and used as test benchmark for different sensitivity schemes in [5,21].

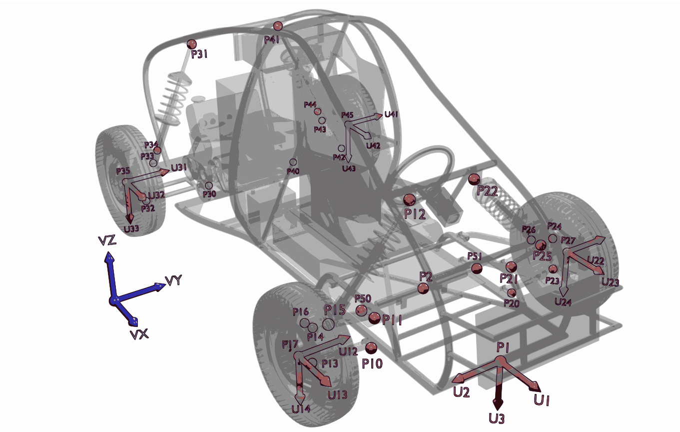

Fig. 2 Points and vectors used to model the four-wheeled vehicle.

The mechanism depicted in figure 2 is composed by 18 bodies and is subjected to gravitational forces, spring-damper forces on the suspensions, contact and frictional tire forces, and to a guidance of the steering rack by means of a rheonomic constraint. The user information referred to points and vectors is translated by MBSLIM into a natural coordinates model of 180 mixed coordinates restricted by 178 constraint equations, and to a relative coordinates model of 36 joint coordinates subjected to 26 constraint equations.

Me maneuver considered consists of a descent of a 1.0 cm step placed at 5.5 m from the initial position in the forward direction of the vehicle. The vehicle has an initial velocity of 3.0 m/s in the forward direction with 11.0 rad/s of spin velocity for each wheel, and there are no additional traction forces.

A measure of driver's comfort is regarded as objective function. It is calculated as the integral over time of the square of the vertical accelerations experimented by the pilot (considered as rigidly attached to the chassis) during the step descent maneuver:

$$\psi = \int_{t_0}^{t_F} \ddot{r}_{1_z}^2 \mathrm{dt} \tag{50}$$

The set of sensitivity parameters selected for this maneuver are:

$$\boldsymbol{\rho} = \left[k_f \ c_f \ k_r \ c_r \ m_c\right] \tag{51}$$

wherein k_f and c_f are the stiffness and damping coefficients of the front suspensions, k_r and c_r denote the stiffness and damping coefficients of the rear suspensions and m_c represents the mass of the chassis.

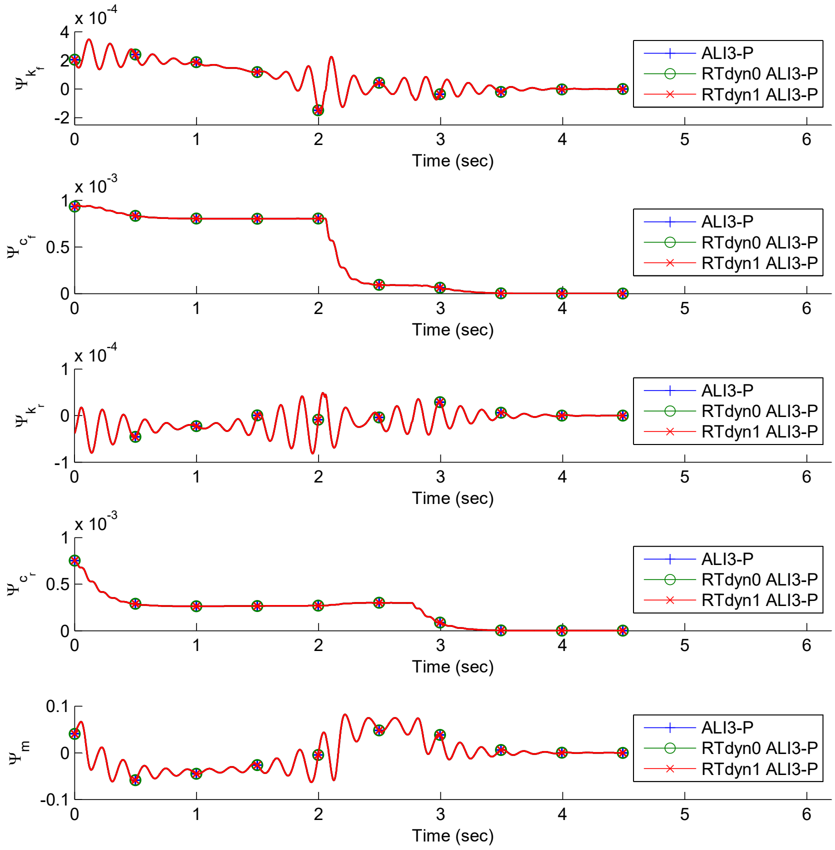

Fig. 3 Evolution of each component of the objective function gradient during the backwards time integration using the DAVM.

Figure 3 represents the evolution of each of the components of the gradient during the backward time integration for the DAVM applied to ALI3-P in natural and relative coordinates. Behold that the value of each component of the gradient at each time step does not represent the real value of the gradient, but only an intermediate integration result. The final results of the gradient are displayed in table 3. Observe that despite the complete different formulations, differentiation methods and sets of coordinates, the DAVM demonstrates an excellent level of accuracy.

	RTdyn0 ALI3-P	RTdyn1 ALI3-P	ALI3-P	Reference
$(\boldsymbol{\psi})'_{k_f}$	2.052e-4	2.054e-4	2.052e-4	2.054e-4
$(\boldsymbol{\psi})'_{c_f}$	9.336e-4	9.336e-4	9.336e-4	9.336e-4
$(\boldsymbol{\psi})'_{k_r}$	-3.843e-5	-3.844e-5	-3.814e-5	-3.814e-5
$(\boldsymbol{\psi})'_{c_r}$	7.532e-4	7.532e-4	7.532e-4	7.532e-4
$(\boldsymbol{\psi})'_{m_c}$	4.060e-2	4.058e-2	4.092e-2	4.090e-2

Table 3 Sensitivities of each component of objective function.

7 Conclusions

In this paper, the application of the DAVM to ALI3-P formulations was accomplished for Newmark's family numerical integrators. The generation of the set of adjoint equations has been funded on the application of the adjoint variable formalism to the discrete expressions of the EoM of a multibody system. As result, 2 accumulation terms $\mathbf{G}$ and $\mathbf{H}$ have been identified as "couplings" between time steps during the backwards integration in time of the adjoint equations.

An special attention has been put on the initial instant of time. The two kinematic position and velocity problems along with the dynamic acceleration problem have been derived and their adjoint equations have been reached.

It has been demonstrated that the DAVM method gathers the advantages of the CAVM, which are a reduced set of variables and systems of equations, with the benefits of DDM, which are the conservation of the order of the time derivatives of the dynamic magnitudes from the original dynamic problem and the straightforward initialization process. As main drawback, the set of equations presented is particular for the Newmark's family integrator, and the use of other numerical integrator will lead to different expressions and to different accumulation terms.

The method has been implemented in the general purpose multibody library MBSLIM for natural and relative coordinate models. Both theory and implementation have been tested with two numerical experiments. First, the sensitivity analysis expressions have been tested in a five-bar mechanism with design parameters in order to test accuracy, and then with control parameters so as to test efficiency. The second experiment consists on the sensitivity analysis of a vehicle during a step decent maneuver. In both experiments, results display a satisfactory level of accuracy with a reduced computational time.

Acknowledgements The support of the Spanish Ministry of Economy and Competitiveness (MINECO) under project DPI2016-81005-P and the support of Spanish Ministry of Science and Innovation (MICINN) under project PID2020-120270GB-C21 are greatly acknowledged. Furthermore, the second author would like to emphasize the acknowledgment for the support of MINECO by means of the doctoral research contract BES-2017-080727, co-financed by the European Union through the ESF program.

References

1. J. Arora, E. Haug. Methods of design sensitivity analysis in structural optimization. AIAA Journal, 17(9):970–974, 1979. doi:10.2514/3.61260.
2. E. J. Haug, J. Arora. Applied optimal design: Mechanical and structural systems. 1979.
3. N. Mani, E. Haug. Singular value decomposition for dynamic system design sensitivity analysis. Engineering with Computers, 1(2):103–109, 1985. doi:10.1007/BF01200068.
4. O. Bruls, P. Eberhard. Sensitivity analysis for dynamic mechanical systems with finite rotations. International Journal for Numerical Methods in Engineering, 74(13):1897–1927, 2008. doi:10.1002/nme.2232.
5. D. Dopico, F. González, A. Luaces, M. Saura, D. García-Vallejo. Direct sensitivity analysis of multibody systems with holonomic and nonholonomic constraints via an index-3 augmented lagrangian formulation with projections. Nonlinear Dynamics, 2018. doi:https://doi.org/10.1007/s11071-018-4306-y.
6. P. Maciag, P. Malczyk, J. Fraczek. Hamiltonian direct differentiation and adjoint approaches for multibody system sensitivity analysis. International Journal for Numerical Methods in Engineering, 121(22):5082–5100, 2020. doi:10.1002/nme.6512.
7. M. Gutiérrez-López, A. Callejo, J. García de Jalón. Computation of independent sensitivities using maggi's formulation. 2012.
8. A. Callejo, D. Dopico. Direct sensitivity analysis of multibody systems: A vehicle dynamics benchmark. Journal of Computational and Nonlinear Dynamics, 14(2):021004–021004–9, 2019. doi: 10.1115/1.4041960.

9. E. Haug. Computer aided optimal design: structural and mechanical systems, chapter Design sensitivity analysis of dynamic systems, 705–755. Number 27 in NATO ASI series. Series F, Computer and systems sciences. Springer-Verlag, 1987. doi:10.1007/978-3-642-83051-8_22.
10. D. Bestle, J. Seybold. Sensitivity analysis of constrained multibody systems. Archive of Applied Mechanics, 62(3):181–190, 1992. doi:10.1007/BF00787958.
11. T. Lauss, S. Oberpeilsteiner, W. Steiner, K. Nachbagauer. The discrete adjoint gradient computation for optimization problems in multibody dynamics. Journal of Computational and Nonlinear Dynamics, 12(3), 2017. doi:10.1115/1.4035197.
12. A. Callejo, V. Sonneville, O. Bauchau. Discrete adjoint method for the sensitivity analysis of flexible multibody systems. Journal of Computational and Nonlinear Dynamics, 14(2), 2019. doi: 10.1115/1.4041237.
13. E. Bayo, R. Ledesma. Augmented Lagrangian and mass-orthogonal projection methods for constrained multibody dynamics. Nonlinear Dynamics, 9(1-2):113–130, 1996. doi:10.1007/BF01833296.
14. D. Dopico, F. González, J. Cuadrado, J. Kövecses. Determination of holonomic and nonholonomic constraint reactions in an index-3 augmented Lagrangian formulation with velocity and acceleration projections. Journal of Computational and Nonlinear Dynamics, 9(4):041006, 2014. doi:10.1115/1.4027671.
15. D. Dopico. Formulaciones semi-recursivas y de penalización para la dinámica en tiempo real de sistemas multicuerpo. Ph.D. thesis, Universidade da Coruña, 2004.
16. D. Dopico, Á. López, A. Luaces. Augmented lagrangian index-3 semi-recursive formulations with projections. Multibody Syst Dyn, 2020. doi:https://doi.org/10.1007/s11044-020-09771-9.
17. J. Cuadrado, R. Gutiérrez, M. Naya, M. González. Experimental validation of a flexible mbs dynamic formulation through comparison between measured and calculated stresses on a prototype car. Multibody System Dynamics, 11(2):147–166, 2004. doi:10.1023/B:MUBO.0000025413.13130.2b.
18. R. Gutiérrez. Cálculo de tensiones en componentes de sistemas móviles mediante dinámica de sistemas multicuerpo flexibles. Ph.D. thesis, Universidade da Coruña, 2003.
19. U. Lugrís. Real-time methods in flexible multibody dynamics. Ph.D. thesis, Universidade da Coruña, 2008.
20. M. A. Naya. Aplicación de la Dinámica Multicuerpo en Tiempo Real a la Simulación y el Control de Automóviles. Ph.D. thesis, Universidade da Coruña, 2007.
21. D. Dopico, A. Sandu, C. Sandu. Adjoint sensitivity index-3 augmented lagrangian formulation with projections. Mechanics Based Design of Structures and Machines, 2021. doi: 10.1080/15397734.2021.1890614.
22. D. Dopico, A. Luaces, U. Lugrís, M. Saura, F. González, E. Sanjurjo, R. Pastorino. Mbslim: Multibody systems in laboratorio de ingeniería mecánica, 2009-2016.
23. J. Orden, D. Dopico. On the stabilizing properties of energy-momentum integrators and coordinate projections for constrained mechanical systems. Computational Methods in Applied Sciences, 4:49–67, 2007. doi:10.1007/978-1-4020-5684-0_3.
24. S. Wang, Q. Tian, H. Hu, J. Shi, L. Zeng. Sensitivity analysis of deployable flexible space structures with a large number of design parameters. Nonlinear Dynamics, 105(3):2055–2079, 2021. doi: 10.1007/s11071-021-06741-4.
25. A. Sandu. On the properties of runge-kutta discrete adjoints. In V. N. Alexandrov, G. D. van Albada, P. M. A. Sloot, J. Dongarra, editors, Computational Science ICCS 2006, 550–557. Springer Berlin Heidelberg, Heidelberg Berlin, 2006.
26. T. Lauss, S. Oberpeilsteiner, W. Steiner, K. Nachbagauer. The discrete adjoint method for parameter identification in multibody system dynamics. Multibody System Dynamics, 42(4):397–410, 2018. doi: 10.1007/s11044-017-9600-9.
27. E. Bayo, J. Garcia De Jalon, M. A. Serna. A modified lagrangian formulation for the dynamic analysis of constrained mechanical systems. Computer Methods in Applied Mechanics and Engineering, 71(2):183–195, 1988.
28. J. M. Pagalday. Optimización del comportamiento dinámico de mecanismos. Ph.D. thesis, Universidad de Navarra, 1994.
29. D. Dopico, Y. Zhu, A. Sandu, C. Sandu. Direct and adjoint sensitivity analysis of ordinary differential equation multibody formulations. Journal of Computational and Nonlinear Dynamics, 10(1):1–8, 2014. doi:10.1115/1.4026492.
30. D. Dopico, A. Sandu, C. Sandu, Y. Zhu. Sensitivity analysis of multibody dynamic systems modeled by odes and daes. In Z. Terze, editor, Multibody Dynamics. Computational Methods and Applications, volume 35 of Computational Methods in Applied Sciences, chapter Sensitivity Analysis of Multibody Dynamic Systems Modeled by ODEs and DAEs, 1–32. Springer, 2014. doi:10.1007/978-3-319-07260-9.
31. Y. Zhu, D. Dopico, C. Sandu, A. Sandu. Dynamic response optimization of complex multibody systems in a penalty formulation using adjoint sensitivity. Journal of Computational and Nonlinear Dynamics, 10(3):1–9, 2015. doi:10.1115/1.4029601.
32. L. Piegl, W. Tiller. The NURBS Book (2nd Ed.). Springer-Verlag, Berlin, Heidelberg, 1997.